

Review

Advances in Biosensor Applications of Metal/Metal-Oxide Nanoscale Materials

Md Abdus Subhan ^{1,*}, Newton Neogi ¹, Kristi Priya Choudhury ¹ and Mohammed M. Rahman ²

¹ Department of Chemistry, Shahjalal University of Science and Technology, Sylhet 3114, Bangladesh; newton@student.sust.edu (N.N.); kristi021@student.sust.edu (K.P.C.)

² Center of Excellence for Advanced Materials Research (CEAMR), Department of Chemistry, Faculty of Science, King Abdulaziz University, Jeddah 21589, Saudi Arabia; mmrahman@kau.edu.sa

* Correspondence: subhan-che@sust.edu

Abstract: Biosensing shows promise in detecting cancer, renal disease, and other illnesses. Depending on their transducing processes, varieties of biosensors can be divided into electrochemical, optical, piezoelectric, and thermal biosensors. Advancements in material production techniques, enzyme/protein designing, and immobilization/conjugation approaches can yield novel nanoparticles with further developed functionality. Research in cutting-edge biosensing with multifunctional nanomaterials, and the advancement of practical biochip plans utilizing nano-based sensing material, are of current interest. The miniaturization of electronic devices has enabled the growth of ultracompact, compassionate, rapid, and low-cost sensing technologies. Some sensors can recognize analytes at the molecule, particle, and single biological cell levels. Nanomaterial-based sensors, which can be used for biosensing quickly and precisely, can replace toxic materials in real-time diagnostics. Many metal-based NPs and nanocomposites are favorable for biosensing. Through direct and indirect labeling, metal-oxide NPs are extensively employed in detecting metabolic disorders, such as cancer, diabetes, and kidney-disease biomarkers based on electrochemical, optical, and magnetic readouts. The present review focused on recent developments across multiple biosensing modalities using metal/metal-oxide-based NPs; in particular, we highlighted the specific advancements of biosensing of key nanomaterials like ZnO, CeO₂, and TiO₂ and their applications in disease diagnostics and environmental monitoring. For example, ZnO-based biosensors recognize uric acid, glucose, cholesterol, dopamine, and DNA; TiO₂ is utilized for SARS-CoV-19; and CeO₂ for glucose detection.

Keywords: biosensors; enzyme-free biosensors; metal-based nanomaterial; metal-oxide nanomaterial; biochip



Received: 4 December 2024

Revised: 25 January 2025

Accepted: 28 January 2025

Published: 3 February 2025

Citation: Subhan, M.A.; Neogi, N.; Choudhury, K.P.; Rahman, M.M.

Advances in Biosensor Applications of Metal/Metal-Oxide Nanoscale Materials. *Chemosensors* **2025**, *13*, 49. <https://doi.org/10.3390/chemosensors13020049>

Copyright: © 2025 by the authors. Licensee MDPI, Basel, Switzerland. This article is an open access article distributed under the terms and conditions of the Creative Commons Attribution (CC BY) license (<https://creativecommons.org/licenses/by/4.0/>).

1. Introduction

A biosensor comprises two coupled segments: a bioreceptor and a transducer [1]. The bioreceptor acts as the recognition element, where the bioreceptor detects and interacts directly with a target analyte. The transducer converts the bioreceptor signal into a quantifiable output that can be evaluated. The receptors of a biosensor are expected to interact with the analytes so that their concentration may be calculated within a range of specificity. Proteins, nucleic acids, and other analytes may be interesting based on their origin [2]. Biosensors are preferred for detecting such analytes compared to other detection approaches, as they are handy, benefit multiple applications, and are less time-consuming. The first biosensor was depicted in a published paper in 1956 [3]. As the biosensor field has expanded, the number of accurate and accessible testing options that do not require

invasive procedures has increased [4]. Recent research has focused on developing biosensors with high sensitivity, selectivity, affinity, simplicity, quick response, and cost-effective analysis [5]. For example, some biosensors can recognize one parasite in a single microliter of blood [6]. As a result, biosensors effectively detect infectious diseases to improve clinical outcomes and promote public health. Advances in biosensor technologies have prospects to bring point-of-care diagnostics to match or exceed the current standard of care regarding time, cost, and accuracy.

Nanotechnology offers potential approaches to address the current limitations of conventional biosensors [7]. Implementing nanotechnologies such as functional nanomaterials, nanoengineering, and nanoplatform fabrication techniques to biosensors is crucial for enhancing the utilization of biosensors. One of the significant advances in experimental design before expanding a nanomaterial into the sensing application is “Nanofabrication”. This progression prompts two significant activities: first, the assembling and designing of nanoscale adhesion using external fields such as electric field-, magnetic field-, optical field-, and fluidic flow-directed assembly, and second, the utilization of micromachining measures for designing nanomaterial surfaces [7,8].

There is a growing demand for early-stage detection of diseases, such as diabetes, chronic kidney disease (CKD), and malignant growth [8]. In recent decades, biosensors have been used in the early detection of such chronic and fatal diseases, with a number of studies on improved biosensors for the rapid and simple detection of analytes [4–7,9]. Combining biosensors with nanofabrication techniques has greatly improved the performance of biosensors as well as expanded the range of sensing targets. This review highlights recent advances in electrochemical, optical, physical, and chemical biosensors and their uses in disease detection. Metal-oxide-based nanomaterials have the aptitude to advance the sensitivity and responsiveness of biosensors. For example, nanowires and nanorods offer a one-dimensional construction that can enable effective charge transfer and sensitivity for biosensing. This review highlights recent advances in electrochemical, optical, physical, and chemical biosensors and their uses in disease detection.

2. Types of Biosensors

Biosensors are classified based on their biological recognition and transduction mechanisms [4]. Here, we describe biosensors, including electrochemical, optical, physical (e.g., piezoelectric and thermal), chemical, and biological sensors [10]. Figure 1 exhibits a schematic of biosensing and Table 1 demonstrates different types of biosensors, their principles, and their applications.

2.1. Electrochemical Biosensors

An electrochemical sensor is based on transducing biochemical events to electrical signals. An electrochemical biosensor is composed of an electrochemical transducer, receptor, and detector. Electrochemical biosensors utilize an electrode as a solid support to immobilize biomolecules and electron movement. Electrochemical biosensors, the most commonly available and widely utilized type among biosensors, are more effective than regular estimation approaches [11–17]. This is because of their instrument affectability, high scope of discovery, simplicity of manufacturing and control, replicability, and minimal expense. Cyclic voltammetry, potentiometry, electrochemical impedance spectroscopy (EIS), amperometry, and differential pulse voltammetry are the electrochemical procedures that are utilized in biosensors [11]. Electrochemical biosensors have been promising in clinical diagnosis, food-processing quality control, and environmental monitoring [12]. An example of a highly successful and commercially available electrochemical biosensor is closed-loop artificial pancreas devices, which are used to detect glucose for the manage-

ment of diabetes. This closed-loop biosensor is used for continuous glucose monitoring and insulin delivery via an extracorporeal shunt [4]. Hence, electrochemical biosensors are widely utilized for the diagnosis and management of diabetes to improve the quality of life of diabetic patients [13].

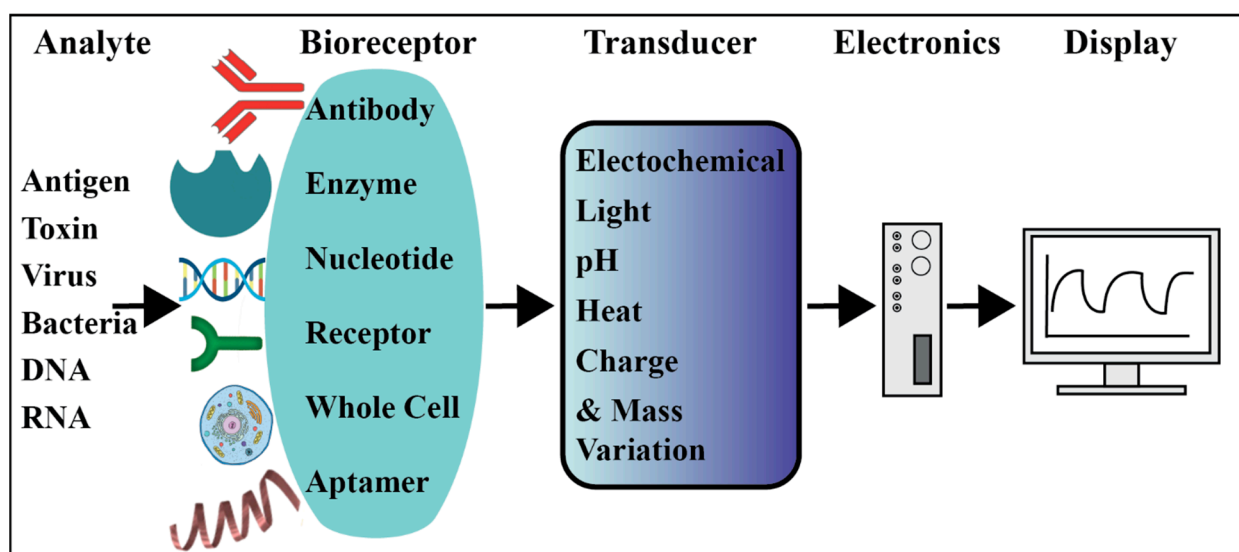


Figure 1. Schematic representation of biosensing. Electronics include read-out technology, amplification, and conversion of signals to digital form.

Various types of nanoparticles, including manganese oxide, titanium dioxide, and nickel oxide, are advantageous candidates for electrochemical sensing. Metal-oxide NPs are low-cost and nontoxic [14]. Additionally, polyaniline (PANI)-TiO₂ nanotubes [15] and ZnO nanostructures have been utilized in developing electrochemical biosensors [16]. ZnO-based electrochemical biosensors have been used for the detection of a variety of analytes such as uric acid, glucose, cholesterol, dopamine, and DNA [17].

Glucose and lactate are both nutrients that fuel our tissues. Lactate is a byproduct of glucose metabolism, which plays a crucial role in human health and disease [18]. The concentration of glucose and, to a lesser degree, lactates, can be dramatically lower than the concentration of dissolved oxygen in the body [19]. As a result, an oxygen deficiency might cause the enzymatic process to be severely stoichiometrically restricted. This oxygen inadequacy/hypoxic condition can be detected by electrochemical biosensors by monitoring reduced glucose levels [20]. Amperometric biosensors are a common method in this category [21]. In separate studies, mesoporous NiO and CuO were utilized for lactate detections [22,23]. NiO/nafion/GCE biosensor for lactate was fabricated utilizing mesoporous NiO with a sensitivity of 62.35 $\mu\text{AmM}^{-1}\text{cm}^{-2}$, detection limits of 27 μM , and detection range of 0.01–27.6 mM [22]. Similarly, using mesoporous CuO, fabricated CuO/nafion/GCE biosensor for lactate detection demonstrated a sensitivity of 80.33 $\mu\text{AmM}^{-1}\text{cm}^{-2}$ [23]. Using an amperometric transduction device, researchers have been able to monitor H₂O₂ using the horseradish peroxidase (HRP) bioreceptor [24]. In the study, PANi-modified platinum terminals were used to immobilize HRPs entrapped in mesoporous silica SBA-15 (SBA-15(HRP)) through electrostatic coupling [24]. An electrochemical biosensor can also be used for the determination of biological oxygen demand in the wastewater [9].

In medicine, electrochemical biosensors have gained much attention over the past few decades for their use in the detection of cancer and other disease biomarkers [25]. In plasma medicine, electrochemical biosensors have been used in various forms including wearable,

implantable, invasive, non-invasive, contact, and non-contact devices [26]. The electronic sensors are fabricated to recognize and quantify different physicochemical parameters such as ion molecules, electrons, antibodies, and enzymes. Electronic sensors are also being used to monitor various parts of the body, such as the heart (electrocardiography), muscles (electromyography), and brain (electroencephalography) [26].

2.2. Optical Biosensors

An optical biosensor is an analytical device that combines a biorecognition sensing element with an optical transducer system. Optical biosensors are well known for their selectivity, sensitivity, and accessibility. These qualities make them ideal for continuously monitoring toxins, drugs, and other microbiologically minute organisms. The sensing mechanism of optical fiber-based sensors is depicted in Figure 2. The sensing mechanism involves exploiting variations in the intensity of light, phase, wavelength, and polarization introduced by the external factors being measured, such as temperature, pressure, strain, and reflective index (Figure 2a) [27]. The optical fiber-based sensor primarily utilizes evanescent waves (EWs) to detect small-scale environmental perturbations. When light propagates through the core of a single-mode fiber, a small portion of EWs penetrates the cladding, facilitating the interaction with surroundings for biosensing. The incident light can be guided using total internal reflection when it strikes the core–cladding interface. A small part of the incident wave penetrates cladding, as shown in Figure 2b. When cladding is partially removed, the EWs interact with the surrounding environment on the etched fiber section, resulting in the change in optical characteristics and enabling the biosensing and detection, as can be seen in Figure 2c [28].

In detecting microbes, optical methods such as surface plasmon resonance (SPR) and resonant mirrors have been utilized. When antibodies against *E. coli* can be immobilized on a Au SPR surface, the maximum number of cells detected at a single spot is 10^6 cells/mL [29].

Optical biosensors are selective and sensitive in monitoring toxins, and pathogenic bacteria. For identifying *E. coli* and *Listeria monocytetes*, it has been demonstrated that utilizing Surface-Enhanced Raman Spectroscopy (SERS) is specific and selective [30], with low detection and quantification limits, 12 cfu/mL and 37 cfu/mL, respectively [31]. An optical fiber biosensor has been developed to detect *E. coli* O157: H7 using a fluorescently tagged aptamer which can specifically distinguish other bacterial strains from *E. coli* strains [32]. In this case, fluorescently labeled aptamers are bound to complementary *E. coli* DNA or probe DNA immobilized on the optical fiber surface, and fluorescent measurements identify *E. coli* [10]. It is possible to detect that even the samples being tested contain fewer instances of *E. coli* if the bright indicator is greater than expected.

A biosensor SiO₂-TiO₂-APTES-PDC-DNA probe was developed to detect *E. coli* in environmental samples [33]. SiO₂-TiO₂ NPs were deposited on a glass substrate and then coupled with APTES, crosslinking the PDC monolayer and the DNA probe. The strands of the DNA probe in the sensor were hybridized with the target DNA strands in *E. coli*, effectively facilitating the *E. coli* detection and measuring the refractive index changes.

A sensitive calorimetric optical aptasensor was fabricated using ZnFe₂O₄-reduced graphene oxide (ZnFe₂O₄-rGO) as an effective peroxidase mimetic to detect *S. typhimurium* [34]. ZnFe₂O₄-rGO NPs were conjugated with aptamers to obtain specific recognition elements. ZnFe₂O₄-rGO NPs catalytically oxidized 3,3',5,5'-tetramethylbenzidine (TMB) by H₂O₂ and produced blue light that was detected by a microreader at 652 nm. The detection range of *S. typhimurium* was 11 to 1.10×10^5 CFU/mL and LOD was 11 CFU/mL [34]. Further, Ag/ZnO/rGO was developed for the detection and killing of *E. coli*. In this nanocomposite, the photocatalytic properties of ZnO, the bacteria-killing and SERS properties of Ag NPs,

and the photothermal conversion properties of rGO were combined to detect and kill *E. coli* effectively [35].

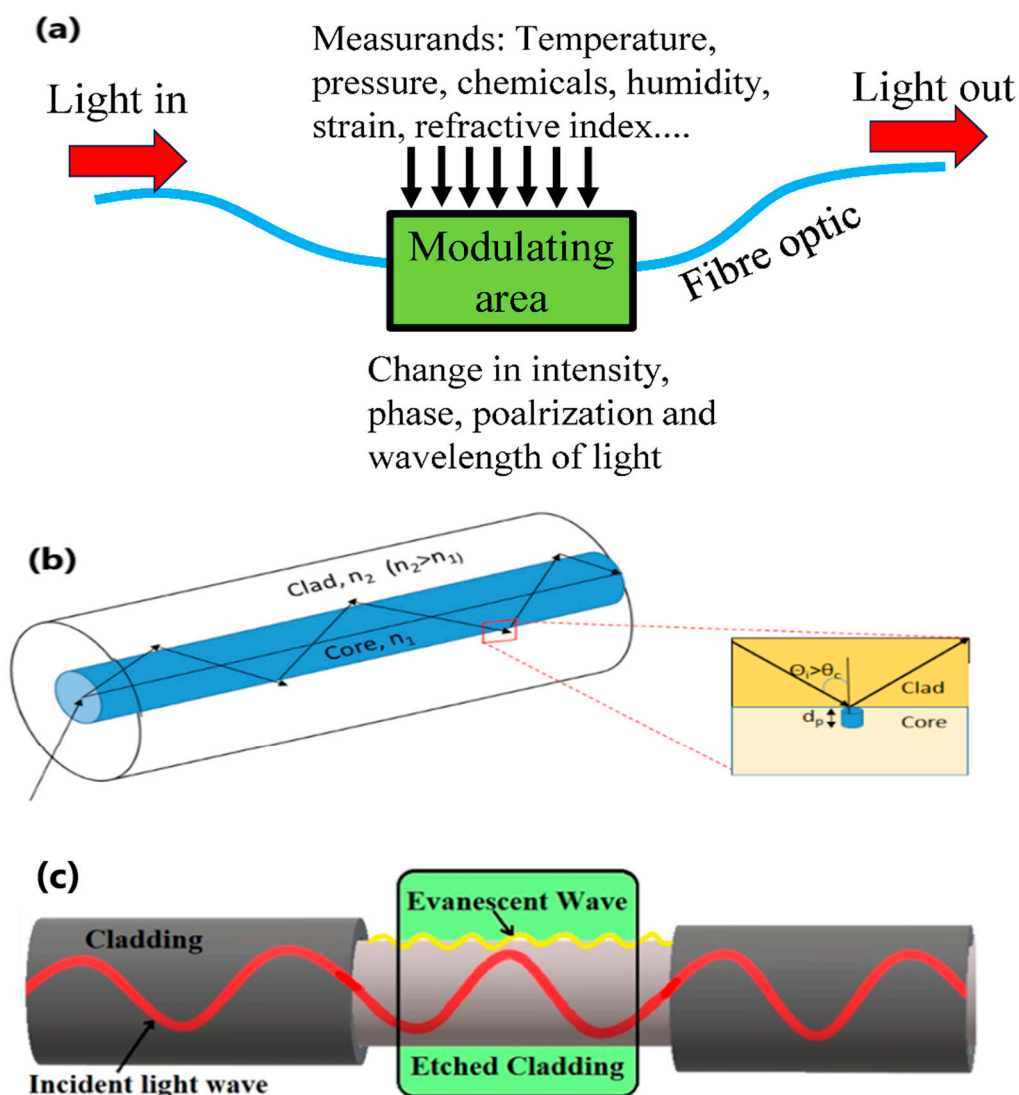


Figure 2. The sensing mechanism of the optical fiber-based sensor; (a) the working mechanism of the fiber optics-based biosensor sensor; (b) the incident light guided by total internal reflection when it strikes the core–cladding interface and a small part of the incident wave penetrates the cladding area with penetration depth d_p ; (c) EWs interact with the surrounding environment on the etched fiber section, resulting in a change in optical characteristics facilitating biosensing; ((a) adapted from [27], and (b,c) adapted with permission from [28] © Optical Society of America/Optica Publishing Group).

A biosensor fabricated using ZnO nanorods coupled with Au NPs (ZnO/Au) coated on the tip of a multimodal plastic optical fiber was utilized for the detection of *E. coli* in polluted water [36]. Au Nps were coated on a transparent plastic optical fiber tip and the ZnO was grown on it through a hydrothermal process to construct the biosensor platform. The sensor showed a fast response within the first 10 s in the presence of polluted water containing *E. coli* with different concentrations ranging from 1000 to 4000 CFU/mL. This sensor platform demonstrated potential in wastewater and food quality monitoring of various pathogenic bacteria [36]. Silver and gold nanoparticles have the potential to revolutionize SERS-based microbial DNA biosensors [37]. Gold NPs exhibit colorimetric changes when they bond with matching DNA, eliminating the need for expensive and labor-intensive fluorescent tagging. As a result, gold NPs are commonly used in bacterial detection equipment, especially for analyzing samples of dark water collected from the

ocean (which absorbs blue light) and from a hypoxic region with low oxygen levels and a minimal number of organisms [10].

ZnO has been used with gold or silver NPs to make efficient biosensors based on SPR and SERS. A thin film of ZnO was deposited on a glass prism coated with Au NPs to detect *Neisseria meningitidis* [38]. The SPR biosensor demonstrated good sensitivity in the range of target DNA concentration from 10 to 180 ng/ μ L. ZnO deposited on the Au surface increased the surface area and SPR signals [36,38]. ZnO was used as a passive component to compensate for losses in optical signal and to enhance the attachment of Au NPs in SPR biosensors [36,38].

rGOs are promising materials for biosensors because they have a high specific surface area, are inexpensive to make, and can interact directly with a wide range of proteins [39]. GO has sp²- and sp³-hybridized carbon atoms and several functional groups like epoxy, carboxyl, hydroxyl, etc. Biomolecules can be stuck to the surface of GO through p-stacking contacts or covalent bonds between the carboxyl groups of GO and the amino groups of biomolecules. GO with specific optical properties has crucial applications in biosensors. It has been established that GO can be used to perform selective biosensing of single-stranded DNA (ssDNA). It has been discovered that ssDNA adsorbs strongly on GO, but duplex DNA (dsDNA) is unable to attach to it stably. It is commonly used in the selective detection of ssDNA in a mixture of other substances (including dsDNA).

Silica fiber is a material that is advantageous in terms of cost, flexibility, and availability. A surface-modified conjugated polymer served as the basis for a biosensor that uses silica microfibers to detect label-free ssDNA targets between pH 1 and 7 [39]. Herein, GO thin film was used as a connecting layer for the adsorption of ssDNA. The selective interaction between GO and ssDNA, which was used as a trap, produced selectivity, and the surface aggregation of ssDNA on the microfiber produced sensitivity [39].

Long-period gratings (LPGs) in optical fiber have been presented as a viable method for label-free biosensors. LPGs are simple to fabricate, robust, and have many of the advantages of optical fibers, such as ease of use, intrinsic small size, high compatibility with optoelectronics, ability for long-distance measurements, and multiplexing. LPGs permit the coupling of the basic core mode to co-propagating cladding modes at well-defined resonance wavelengths because of periodic refractive index (RI) disturbances created in the core of a single-mode optical fiber [40,41]. The transmission spectrum of an LPG can be characterized through one or more attenuation bands, where the minimum of each band corresponds to the coupling with a specific mode when the phase-matching requirement is fulfilled, as stated by the characteristic equation of LPGs, $\lambda_{\text{res}(m)} = (\eta_{\text{eff,core}} - \eta_{\text{eff,clad}(m)})\Lambda$, where Λ is the grating period (usually range from 100 to 600 μ m), $\eta_{\text{eff,core}}$ and $\eta_{\text{eff,clad}(m)}$ represent the effective RIs of fundamental core mode and m -th cladding mode, respectively; $\eta_{\text{eff,clad}(m)}$ depends on the RI of the surrounding medium [40].

SPR using fiber optics is a type of label-free optical biosensor. In label-free detection, the detected signal is generated directly with the on-site interaction of the analyte and the respective transducer. As a result of its adaptability to downsizing and remote-sensing capabilities, it may be put into many hard-to-reach situations for in situ detection as a hand-held probe or as a collection of remotely controlled devices installed at various points along a fiber-optic cable. The most prevalent fiber-optic SPR sensors are composed of unclad, side-polished, tapered, U-shaped optical fibers coated with a nanometric coating of gold or less frequently silver. The fiber grating technology is based on tilted fiber Bragg grating (TFBG). A tilted TFBG sensor, created by tilting the diffraction grating of the FBG sensor at a slight angle, can measure temperature and strain simultaneously without an additional sensor. It can also measure the refractive index around the sensor, the degree of resin hardening, bending deformation, humidity, torsion, etc. The TFBG sensor is a

multifunctional sensor [42]. The TFBG has been created to fabricate a highly efficient SPR sensor with several distinct benefits. This sensor offered an extra resonant mechanism of high-density, narrow-mode spectral combs at near-infrared wavelength (with a spectral width of the resonance between 0.01 and 0.1 nm). Thus, it overlapped with the surface plasmon's wide absorption for high-precision investigation. It increased the RI resolution from 106 to 108 refractive index units. This provided a linear RI response in both liquids and air. The TFBG sensor's mechanical resistance is slightly affected. Using well-established phase masks for grating inscription, its mass manufacturing with high repeatability is simple to perform [43]. Coating TFBGs with indium tin oxide (ITO) enabled them to be used in a variety of applications. Enhanced leaky mode resonances (eLMR) correspond to the high-order modes with an effective refractive index (ERI) that is smaller than the surrounding refractive index (SRI). These modes exhibit very different characteristics compared to those of cladding modes, SPR, and lossy mode resonance (LMR), and they have the potential to become the third type of resonance associated with optical fiber coated with thin films. This type of resonance is characterized by a high real part of the complex RI of the material. Recent research has resulted in the development of two distinct applications that make use of the same sensor arrangement. The first aspect is referred to as the use of birefringence in ITO-coated TFBGs, which makes it possible to create a device for detecting vector twists. The latter term refers to an in-fiber linear polarizer that has a comb-like structure and is based on leaky mode resonances in ITO-coated TFBGs. Enhancing the mode coupling with the guided mode is accomplished by the thin film's ability to induce the guiding of S-polarized leaky modes. By tweaking the specifications of the device, it was possible to achieve both a spectacular polarization extinction ratio and an extremely narrow bandwidth [44]. Figure 3 demonstrates an ITO thin film-coated TFBG sensor consisting of four layers, including a fiber core where the tilted grating is inscribed, fiber cladding, ITO coating, and the external environment. The input light polarized in p- or s-states (as indicated by P and S in Figure 3) was launched into the fiber core to excite the p- or s-polarized core-guided mode that couples with cladding-guided modes, leaky modes, and even with the lossy modes in the tilted grating regions. The output light is then collected at the other end of the fiber core to generate the resonance, including the cladding mode resonance and eLMR (enhanced lossy mode resonance), in the transmission spectrum. LMR may be generated if the condition is satisfied. Leaky modes are essentially highly lossy in bare optical fiber due to the large imaginary part of the ERI, and they can not propagate through the waveguide. They could become guided similarly as a surface wave, only when the imaginary part of ERI is reduced. In that case, the core-guided mode will interact with guided leaky modes within its propagation to generate eLMR. The eLMR, LMR, and SPR are dependent on leaky modes guided in optical fiber, lossy modes guided in nanocoating, and SPR modes guided in nanocoatings (commonly metal films only). eLMR can be effectively excited by s-polarized light while p-polarization demonstrates little variations. SPR can only be excited by p-polarized light. LMR can be excited by both s- and p-polarized light. The LMR represents the highest sensitivity evaluated by the wavelength shift. The SPR has lower sensitivity, but SPR-based devices have received an exponential increase during the last 2–3 decades. The eLMR is a relatively new optical sensor with increased performance. The eLMR excited in TFBG has the narrowest FWHM among these three resonance, indicating that the q-factor can be greatly improved [45].

Over the last two decades, the study of meta-materials has been the focus of progressively growing attention in several different scientific groups. This leads to the demonstration of strange phenomena such as invisibility cloaking, negative refraction, and superlensing. Their 2D analogs, commonly called "meta-surfaces" (MSs), have been the subjects of active study owing to several benefits. This is because 2D MSs are easier to work with

than 3D counterparts [44]. A ‘Lab-on-Fiber’ (LoF) optrode based on phase-gradient plasmonic MSs integrated on the tip of an optical fiber can potentially outperform plasmonic benchmarks in biological systems for the detection of nanoscale molecular interactions [46].

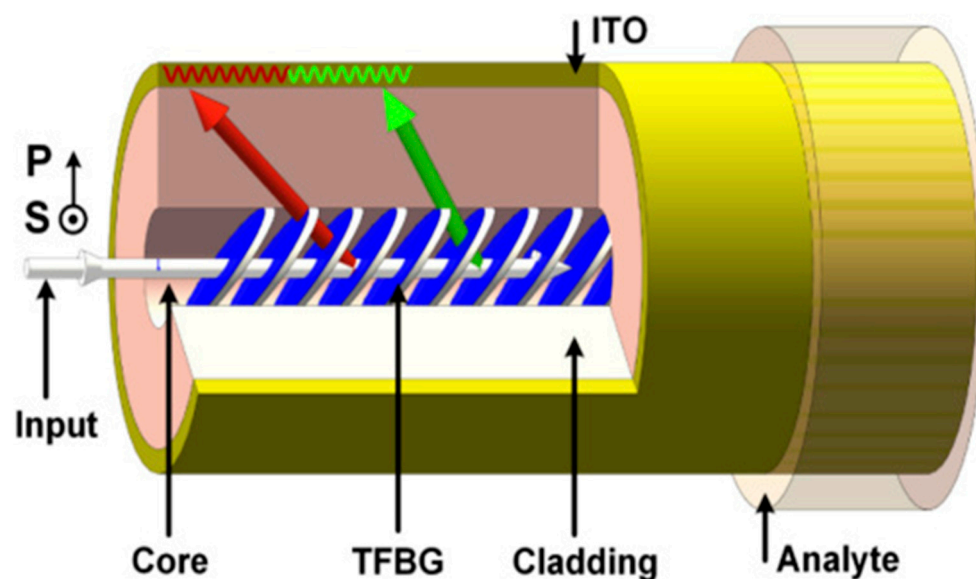


Figure 3. Schematic diagram of ITO-nanocoating-integrated TFBG sensor (adapted from [45]).

C-reactive protein (CRP), a biomarker implicated in various illnesses and the subject of substantial research, was used as an example analyte to evaluate the performance of a fiber-optic-based label-free biosensor [47]. The device is based on a long-period grating constructed in a double-cladding fiber with a W-shaped RI profile. The fiber transducer was coated with a nanometric-thin GO layer to provide functional groups for covalently immobilizing the biological recognition element. A meager detection limit (0.15 ng/mL) was achieved for detecting CRP in serum with a large working range of clinical relevance, 1 ng/mL–100 µg/mL [47]. Age, gender, smoking status, weight, cholesterol levels, and blood pressure may alter the serum CRP level, which is expected to be 0.8 g/mL in healthy Caucasians. In some bacterial infections, CRP, a blood biomarker of infection or inflammation, can rise 1000-fold [24]. Devices that are based on optical fiber are beneficial for CRP detection, and because of their micro-sized cross-sections, they are excellent for minimally invasive procedures as well as in vivo procedures for the detection of CRP [48].

Alzheimer’s disease (AD) is one of the most severe neurological conditions. Stroke is associated with AD among elderly people, and the relation is strongest in the presence of known vascular risk factors [49].

Table 1. Principles and applications of different types of biosensors.

Sensor Name	Principle	Sensing Elements	Transducers	Application	Refs.
Glucose oxidase electrode-based	Electrochemistry using glucose oxidation	Glucose	Cuprophane–glucose oxidase—Cuprophane membrane and a pH electrode.	Analysis of glucose in biological Sample	[50,51]
HbA1c	Electrochemistry using Ferrocene boronic acid	Hemoglobin	Ferroceneboronic acid (FcBA)	Glycated hemoglobin measurement using a robust analytical technique	[52]
Uric acid	Electrochemistry	Uric acid	Enzymatically generated H ₂ O ₂	Detection of illnesses or clinical abnormalities	[53]
Acetylcholinesterase inhibition-based	Electrochemistry	Pesticide	Acetylcholinesterase	Understanding pesticidal impact	[54]
Piezoelectric	Electrochemistry	Pesticides	Cholinesterase (ChE) Molecular imprinting polymers (MIPs)	Identifying carbamate and organophosphate	[55]

Table 1. Cont.

Sensor Name	Principle	Sensing Elements	Transducers	Application	Refs.
Microfabricated	Optical/visual biosensor using cytochrome P450 enzyme	Cholesterol	Cytochrome P450 Enzyme microfabricated electrodes	Pharmaceutical research and development	[56]
Hydrogel (polyacrylamide)-based	Optical/visual biosensor	DNA	DNA-functionalized hydrogels	Biomolecular immobilization	[57]
Silicon	Optical/visual/fluorescence	DNA	Sandwiched-structured Silicon nanowire	Bioimaging, biosensing, and cancer therapy	[58]
Quartz-crystal	Electromagnetic	Protein	Wireless-electrodeless QCM	Ultrasensitive protein detection in liquids	[59]
Nanomaterials-based	Electrochemical or optical/visual/fluorescence	Enzyme	Gold-NPs	Diagnosis and Therapy	[60]
Genetically encoded or fluorescence-tagged	Fluorescence	ADP and ATP	ATPase	Evaluation of the biological processes, which include numerous molecular systems inside the cell	[61]
Microbial fuel cell-based	Optical	Pesticides	<i>Chlorella vulgaris</i> coupled optic fiber signal	Environmental monitoring of biochemical oxygen demand and toxicity, and heavy metal and pesticide toxicity	[62,63]

The early detection of AD is necessary for accurate prognosis, treatment, and monitoring. The affordability and ease of use of biomarkers distinguish them for early AD screening. RI-sensitive metal-oxide biosensors may be effective in the early detection of AD. In cutting-edge applications, optical sensors are becoming more prevalent. Fiber-optic sensors provide exceptional light control. Light from a photonic device interacts with its environment to generate surface waves. The evanescent field analyzes all medium changes in surface waves by measuring RI. Nano LoF sensor systems and nanoparticles, nanofilms, or nanostructures modify the interaction between light and matter with astounding resolution, precision, and accuracy, thus offering an image of technologically advanced, ultrahigh-performance optical systems. The transmission spectrum of the sensor reveals that biological changes at the fiber surface influence the surface RI, which has a significant impact on the optical properties of the LMR. Existing resonance-based optical technology platforms are surpassed by the adaptability and advantage of LMR detection [50]. SPR is a well-known thin-film-sensing phenomenon. The nanocoating must have a complicated RI to generate this resonance. LMR bands in a well-defined wavelength range described the transmission spectrum of an LMR-based sensor [51]. LMRs are less well known than SPRs, but they have many interesting features, such as the ability to tune the resonance position at any wavelength in the optical spectrum by controlling the nanocoating thickness and the ability to complement metallic materials typically used in SPR-based sensors with polymers and metallic oxides [52]. LMR has many advantages over SPR, such as easy wavelength tuning in the optical spectrum as a function of coating thickness, cheaper coating material, the ability to excite both transverse electric (TE) and transverse magnetic (TM) light polarization states, and multiple LMR generation. To have a particularly sensitive response in LMR, the waveguide modes must be matched with a lossy mode of the semi-conductor nanocoating, and an optimal film thickness may enhance transmission spectrum attenuation [53]. Sensors based on LMR need nanocoating thickness control and characterization. SnO₂ nanomaterials are most RI-sensitive and LMR-exciting [54]. The LoF biosensor utilized SnO₂ for the specific detection of Tau protein as one of the AD biomarkers that are highly correlated with AD progression in cerebrospinal fluid with a detection limit of 10⁻¹² M and over a wide concentration range (10⁻³ to 10 μg mL⁻¹). The LoF, SnO₂-based sensors are promising for the rapid and highly sensitive detection of Tau proteins at low concentrations, which may be a potential approach for early screening and personalized medicine for AD patients [50].

A sensitive plasmonic photonic crystal fiber (PCF) was reported for cancer cell detection by measuring RI [55]. PCF sensor was fabricated with dual V-shaped grooves to enhance the sensor activity where two AuNRs were mounted on the etched surfaces. A RI optical sensor was utilized to track the electromagnetic coupling between the leaky core mode (LCM) and the surface plasmon mode (SPM) at the metal/dielectric interface. When the SPM and one of the fundamental core modes are phase-matched, a strong coupling occurs. The maximum confinement was achieved for the core-guided mode at the resonance wavelength, which is dependent on the analyte RI. The V-shaped groove increased the core/SPM coupling, where a high RI sensitivity of 24,000 nm/RIU was achieved in an RI range from 1.38 to 1.39 with a resolution of 2.73×10^6 RIU. Good sensitivities of 23,700 nm/RIU, 8208 nm/RIU, and 14,428 nm/RIU were achieved for basal, cervical, and breast cancer cells with resolutions of 4.22×10^6 RIU, 12.18×10^6 RIU, and 6.93×10^6 RIU, respectively. In this approach, the RI measured for normal and cancer cells for basal (1.360/1.380), cervical (1.368/1.392), and breast cells (1.385/1.399) were distinguishable and suitable for cancer detection. The RI cancer sensor demonstrated good sensitivity and resolution as well as a good fabrication tolerance of 5% for fabrication imperfection. Label-free sensors are safer than chemical and surgical approaches [55].

Optical biosensors with metal oxides perform better in sensing biological samples in clinical diagnostics [56]. Various types of optical biosensors utilizing metal-oxide NPs have been used for the detection of numerous biological entities including serum ferritin, H_2O_2 , IgG, nucleic acid, and glucose [56]. A nanoplatfrom based on titanium dioxide nanotubes and TiO_2 NT/alginate hydrogel scaffold was developed for lactate and glucose monitoring in artificial sweat. The sensing time for glucose and lactate were 6 min and 4 min, respectively. The biosensor platform was utilized for the detection of glucose and lactate in a concentration range of 0.1–0.8 mM and 0.1–1 mM. The sensor TiO_2 NT/alginate hydrogel scaffold platform used calorimetric optical signal (blue color) detection in sweat samples. The sensor TiO_2 NT/alginate hydrogel scaffold was integrated into the paper substrate to enhance the sensing performance [56].

3. Piezoelectric Biosensor

Piezoelectricity is the ability of a material to create an internal electric field when a mechanical stress or strain is applied. Piezoelectric materials may be crystal, ceramic, or polymer films, such as aluminum phosphate or nitride, ZnO, or quartz (SiO_2). An alternating voltage is applied to piezoelectric materials between two electrodes in biosensing. The oscillation frequency of a piezoelectric material changes according to mass bound to the electrode or the medium viscosity. For example, a piezoelectric response is observed when an antigen that binds to an antibody immobilizes on the electrode surface [57].

Piezoelectric biosensors have been used to detect small molecules and ions in biological samples. One such biosensor, developed by covalently linking metallothionein and quartz crystal, has been used to monitor Zn^{2+} and Cd^{2+} in fluid media, such as phosphate buffer and tetraborate buffer [58].

Quartz crystal microbalance (QCM) has been used in the development of a piezoelectric nano-biosensor for accurate Hg^{2+} detection. The detection component of this system is made up of three different kinds of DNA assays, each of which includes reporter DNAs linked to NPs. The particular T- Hg^{2+} -T (T = thymine) complex has been gathered by Hg^{2+} stacking because this complex could not be hybridized with functionalized NPs. Due to the higher concentration of Hg^{2+} , there was a decrease in the NP-induced improved QCM-Dw reaction. This has the consequence of the reduction in the hairpin formation by the linker DNA [59–62]. Similarly, a DNA enzyme-based QCM-D biosensing instrument demonstrated high affinity and selectivity toward Pb^{2+} [61]. Nanosensors utilizing AlGaIn/GaN

HEMTs (high electron mobility transistors) have been fabricated to monitor different ions. These sensors are sensitive to charges at the surface without requiring a reference electrode. Devices covered with plasticized poly(vinyl chloride) (PVC)-based layers containing an ionophore can be utilized to identify Hg^{2+} and Ca^{2+} ions in water [10]. Temperature and pH are also detected by different methods including the piezoelectric approach [26].

Lymphocytes (B, T, and NK cells) and immunoglobulins are vital for the adaptive immune response against external pathogens. A gold NP (AuNP)-doped polyaniline nanofiber (Au/PANI-NF) composite was fabricated to monitor T cell activation [51]. Anti-CD antibody (Ab) molecule was immobilized onto the composite to observe the expression of CD69, CD25, and CD71, which are T-cell surface activation markers, at the early, middle, and late stages at 8 h, 24 h, and 48 h, respectively, after stimulation of the T cell. EIS measurement demonstrated a limit of detection (LOD) of 10^4 cells/mL. The Au/PANI-NF sensor exhibited a higher LOD than other electrochemical biosensors that are used to monitor the T cells [63].

Zhao et al. reported on nanowire sensors to detect IgG in buffer solution [64]. Piezoelectric ZnO nanowires were vertically grown onto a Ti plate (first electrode) and then coated with a SiO_2 layer. The surfaces of SiO_2/ZnO nanowires were modified with AuNPs and anti-IgG. An Al foil on top of the nanowire was the second electrode. Observations have been made regarding the fluctuations in the surface-free carrier density of nanowires caused by the adsorption of antigens. This shift in the free-carrier density can be utilized to gauge the concentration of antigens. Piezoelectric biosensors exhibit potential in the monitoring of small molecules or ions in biological fluids, as well as biomolecules.

4. Thermal Biosensors

A thermal biosensor is based on the measurement of total heat energy absorbed or produced or the temperature change in a system. Thermal biosensors utilize a flow injection analysis approach using an immobilized enzyme reactor, organized with a differential temperature measurement across the enzyme reactor [65]. The configuration incorporates a pair of thermal transducers, such as thermopiles or thermistors, across the enzyme column packed with immobilized enzymes to alter a substrate to a product [66]. Thermopiles or thermistors are the two commonly utilized thermal sensors. Thermopiles measure the temperature difference between two regions. Thermopiles are a set of thermocouple junctions in series made from metals, semiconductors, and various substrate semiconductor components. The thermistor is a sensitive temperature transducer, which depends on the variations in electric resistance with temperature from which the absolute temperature can be determined but with a limited sensitivity [66]. Bimetallic strips, liquid–gas expansion, pyroelectric systems, metal resistance, and microelectromechanical systems are also used as thermal transducers. Furthermore, highly sensitive thermocouples are an outstanding substitute for detecting temperature changes [67].

Thermal biosensors are now being used to determine the chemical oxygen demand (COD) of H_2O and wastewater utilizing a biosensing device that detects temperature variations. To investigate the COD qualities, periodic acid solutions may be used as oxidants, and flow injection testing equipment can be utilized. This detecting system can deliver a broad range for the sensing of COD in H_2O derived from a variety of sources. The calorimetric COD determination strategy provides more feasible identification outcomes than the standard approach in terms of strength, long-term solidity, and speed [11,65,67].

5. Chemical and Biological Sensors

Different promising nano-structural metal-oxide NPs (MONPs) exist for specific and selective biosensor applications. Engineered MONPs are among the most widely used man-

ufactured materials for their unique properties. MONPs and their potential for chemical and natural gas detection applications have been thoroughly studied [68–71]. Addressing the future financial and social necessities, shrewd determination, planning, and use of MONPs will prompt another age of detecting devices displaying novel capacity alongside improved sign enhancement and coding methodologies [68–70].

A chemical sensor is a device that facilitates communication between the analytical gases or fluids and the sensor. This communication converts chemical or biochemical information into a useful signal, either quantitative or qualitative. The transducers in the sensor device generate signals that are typically electrical. Chemical sensors have a few highlights like steadiness, selectivity, affectability, reaction and recuperation time, and immersion [68]. While the surrounding gases respond with the oxygen in the oxide at high temperatures, the changes in surface potential and resistivity occur as a result. In addition, metal-oxide-based chemical sensors can be utilized in clusters permitting the detection of numerous species with high affectability and low detection limits around ppm levels for certain species. Tin oxide-based chemical sensors, with various morphologies, high affectability, and quick reactions, can recognize hydrogen (H_2) on the SnO_2 NWs surfaces [71,72]. Further, semiconducting metal-oxide gas sensors are effectively utilized for environmental gases (e.g., CO_2 , O_2 , O_3 , and NH_3), highly toxic gases (e.g., CO , H_2S , and NO_2), combustible gases (e.g., CH_4 , H_2 , and liquefied petroleum gas), and volatile organic compound gases. These sensors are effective in monitoring the gaseous markers in the breath of patients for diagnostic and monitoring purposes, as well as for controlling environmental pollution [73,74].

6. Why Metal-Oxide Biosensors?

Nanostructured metal oxide offers an effective surface for biomolecule immobilization with desired orientation, conformation, and biological activity, resulting in improved sensing features and providing a biocompatible environment [75,76]. Nanostructured metal oxides with unique electrical, optical, and molecular properties along with anticipated functionalities and surface charge properties afford suitable platforms for interfacing biorecognition elements with transducers for signal amplification. Metal-oxide-based nanowires and nanorods with a one-dimensional design are suitable for efficient charge transfer and signal transduction. Quantum dots aid particular signal amplification and multiplexing, providing additional sophistication in biosensor technology. Strategies have been implemented to enhance the performance of nanostructured metal-oxide-based biosensors with versatile podiums for functionalizing them for clinical and non-clinical applications. These nanostructured metal oxides have demonstrated many crucial applications in a new generation of miniaturized biosensing devices [75,76]. Here, we emphasized the development of biosensors based on metal-oxide nanoscale materials, including ZnO , TiO_2 , and CeO_2 , and their applications in medical diagnostics and environmental sensing.

6.1. Biosensors Based on Metal-Oxide NPs

MONPs have been utilized in the fabrication of biosensors due to their potential and versatility in modifying their morphology, chemical stability, and physicochemical interfacial properties [73]. MONPs can be assembled into heterostructures, hybrid structures, and composite structures, with innovative electrochemical properties that can be modified for a specific biosensor application. MONP-based biosensor devices consist of sensitive biometric elements, transducers, and signal analysis systems permitting the fast detection of various trace-level analytes. The recognition element can react with (enzyme-based) or bind with (antibody-based) analytes depending on the sensing molecule used. Consequently, the transducer captures the results of the interaction between the recognition elements and the

analyte, in the form of the number of transferred electrons, in the case of redox enzymes, or changes in mass or potential. The chemical modification of MONP biosensors allows for a wider range of detection of various biomolecules [73]. MONP biosensors may be suitable for extended lifetime, stability, and reliability of sensor signals. Further, metal-oxide-based thin-film transistors (TFTs) may contribute to the environmental sensor and automation biosystems [77]. The chemically modified metal-oxide biosensors may be nanoparticles like ZnO, MgO, NiO, TiO₂, CoO, and WO₃, which are used in biosensor devices to detect biomolecules [78,79] (Table 2). They can improve signal and biomolecule immobilization in new in vivo biosensing devices [80]. The bioactive recognition element is connected to the transducer using different methods [81]. A DNA/CeO₂-NP-based fluorometric sensing framework has been developed for the detection of H₂O₂ [82].

CuO is a transition metal oxide with excellent physiochemical properties at the nanoscale, making it a desirable candidate for biosensing. It offers strong electrochemical activity, high surface area, adequate redox potential, and solution stability. CuO nanoparticles can facilitate faster electron transfer on an electrode, making it an excellent platform for glucose electro-oxidation. Various types of CuO nanoparticles have been used to enhance the glassy carbon electrode, enabling nonenzymatic glucose detection in alkaline conditions [83].

ZnO is used in fabricating electrochemical biosensors due to its high isoelectric point, which allows for a simple and more grounded binding of different biomolecules on its surface, its great biocompatibility, and its quick charge-transfer properties. ZnO is a delicate optical and piezoelectric biosensor because of its fluorescence and piezoelectric properties. ZnO-based platforms can be used as an immobilization matrix to build electrochemical biosensors for the discovery of biologically significant analytes such as DNA, metabolites, cancer markers, and so on, and can have clinical implications [84]. ZnO NP-based biosensors have been successfully developed to sense glucose [85,86], xanthine [87], DNA [88], lactate [89], cholesterol [90–92], N-Acyl Homoserine Lactone [93], uric acid [94], epinephrine [95], and urea [96]. Additionally, poly(glutamic acid)/ZnO nanoparticles [97], ZnO NP film [98], and ZnO/chitosan-graft-poly(vinyl alcohol) core-shell nanocrystals (NCs), are utilized as glucose sensors [99]. ZnO NPs–polypyrrole film has been utilized in developing a biosensor that can sense hemoglobin [100]. ZnO NP-based biosensors have been developed to sense acetylcholinesterase (AChE) [101]. AChE is an important enzyme that plays a crucial role in the transmission of nerve impulses mediated by ACh. Any abnormal change in its activity can disrupt neurotransmission and lead to neurodegenerative disorders [102–104]. Researchers have developed ZnO nanoparticles to study AChE activity, which is affected by Cd²⁺ at different concentrations [105]. MgO nanostructures are utilized for the sensing of ascorbic acid, dopamine, and uric acid [106,107]. CuO nanoparticles can sense glucose [108]. CeO₂ nanostructures are also utilized in sensing glucose [109–112], DNA [113], uric acid [114], and concanavalin A [115]. SnO₂ nanofibers [116] and carbon nanotubes@SnO₂-Au composite [117] have activity as glucose sensors. Fe₃O₄ NPs can sense tetracyclines [118], glucose [119–122], coliforms [123], and tyrosinase [124].

Table 2. Different types of biosensors using metal-oxide NPs.

Metal Oxide	Target	Biosensor Type	Transducer	Refs.
SnO ₂ NPs	Glucose	Electrochemical	PANI/SnO ₂ -NF/HRP-GOx/Ch/GC electrode	[116]
	Glucose	Electrochemical	TiO ₂ -GR/GOD colloid dropped glassy carbon electrode (GCE)	[125]
TiO ₂ NPs	Alpha-Synuclein	Photoelectrochemical immunosensor	Au-doped TiO ₂ nanotube	[126]
	PEC-based DNA	Photoelectrochemical	CA-modified TiO ₂ photoelectrodes	[127]
	Organophosphate pesticides	Electrochemical	Chitosan (CS) film-modified TiO ₂ -CS hydrogel	[119]

Table 2. Cont.

Metal Oxide	Target	Biosensor Type	Transducer	Refs.
CeO ₂ NPs	Glucose	Photoelectrochemical	CeO ₂ @MnO ₂ core-shell hollow nanosphere	[128]
	Uric acid	Electrochemical	In doped CeO ₂ NP-modified glassy carbon paste electrode	[129]
	Concanavalin A	Electrochemiluminescence	CeO ₂ @Ag NPs modified graphene quantum dots	[115]
ZnO NPs	DNA	Electrochemical	CeO ₂ -ZrO ₂ NCs on gold electrode	[128]
	Xanthine	Electrochemical	XOD/ZnO-NP/chitosan/carboxylated-MWCNT/PANI/Pt electrode	[87]
	Acetylcholinesterase	Electrochemical	ZnO NPs-CGR-nafion (NF) modified glass carbon electrode (GCE)	[130]
	Glucose	Electrochemical	Graphene (GR)-CNT-ZnO composite modified GCE	[131]
	DNA	Electrochemical	Ionic liquid/ZnO NPs/chitosan/gold electrode	[88]
	Lactate	Electrochemiluminescence	GCE/nanoZnO-MWCNTs (multiwall CNTs)/LOx/NF	[89]
	Cholesterol	Voltammetric	MWCNT-ZnO NPs	[90]
	N-Acyl Homoserine Lactone	Photoluminescence	Cysteamine functionalized ZnO NPs	[71]
	Uric Acid	Electrochemical	Enzyme electrode modified by ZnO NPs and MWCNT	[94]
	Epinephrine	Electrochemical	ZnO NPs/1,3-dipropylimidazolium. Bromide ionic liquid-modified carbon paste electrode	[95]
MgO NPs	Urea	Electrochemical	Nano-ZnO/ITO film-based electrode	[96]
	Ascorbic acid	Electrochemical	MgO nanobelts/GCE	[132]
	Dopamine	Electrochemical	MgO nanobelt-modified graphene-tantalum wire electrode	[133]
	Uric acid	Electrochemical	MgO nanobelts/GCE	[132]
	Glucose	Electrochemical	GE/MgO/glucose oxidase (GOx)/nafion electrodes	[108]
Fe _x O _y NPs	Tetracyclines	Colorimetric	Fe ₃ O ₄ NPs	[118]
	Glucose	Potentiometric	Fe ₃ O ₄ -enzyme-Ppy NPs on magnetic glassy carbon electrode (MGCE)	[121]
	Coliforms	Tyrosinase (Tyr)	Tyr/Fe ₃ O ₄ NPs-CNTs/GCE	[126]

Various TiO₂ NPs have shown promising biosensor applications. TiO₂-graphene composite [125], silver-Prussian blue-modified TiO₂ nanotube array [134], nanocrystalline TiO₂/Au/glucose oxidase films [135], and TiO₂/APTES cross-linked to carboxylic graphene [125] have been used to fabricate glucose sensors. A photoelectrochemical (PEC) biosensor, fabricated utilizing a caffeic acid (CA)-modified TiO₂ photoelectrode, was developed to detect DNA in a concentration range of 100 nM to 1 pM, and with a limit of detection 1.38 pM [127]. Another TiO₂-based sensor, for detecting organophosphate pesticides, was developed by inserting Au nanorod@SiO₂ NPs into a TiO₂-chitosan hydrogel [136]. A self-assembly of a monolayer to introduce oligomeric DNA on the contact layer is crucial for a DNA sensor, as shown in Figure 4. Herein, the surface of TiO₂ NPs was terminated by a hydroxyl group that attached the molecule through a condensation reaction. The transducer was salinized by APTES, which modified the TiO₂ layer by the hydrolyzation of the -OH group on the surface of the TiO₂ NPs and formed siloxane bonds (Si-O-Si) to immobilize the DNA at the surface of the TiO₂ NPs. The silane layer over TiO₂ NPs was thin and uniform, suitable for DNA immobilization on it. The salinization of TiO₂ NPs, and the immobilization of DNA on salinized TiO₂ NPs, are demonstrated in Figure 4 [136]. Further, photochemical DNA sensing on the TiO₂ NP surface by DNA probe immobilization on the catechol-modified TiO₂ NPs in the presence of ascorbic acid generated a photocurrent that decreased following the target DNA hybridization due to steric hindrance aiding the DNA detection, as can be seen in Figure 4b [126].

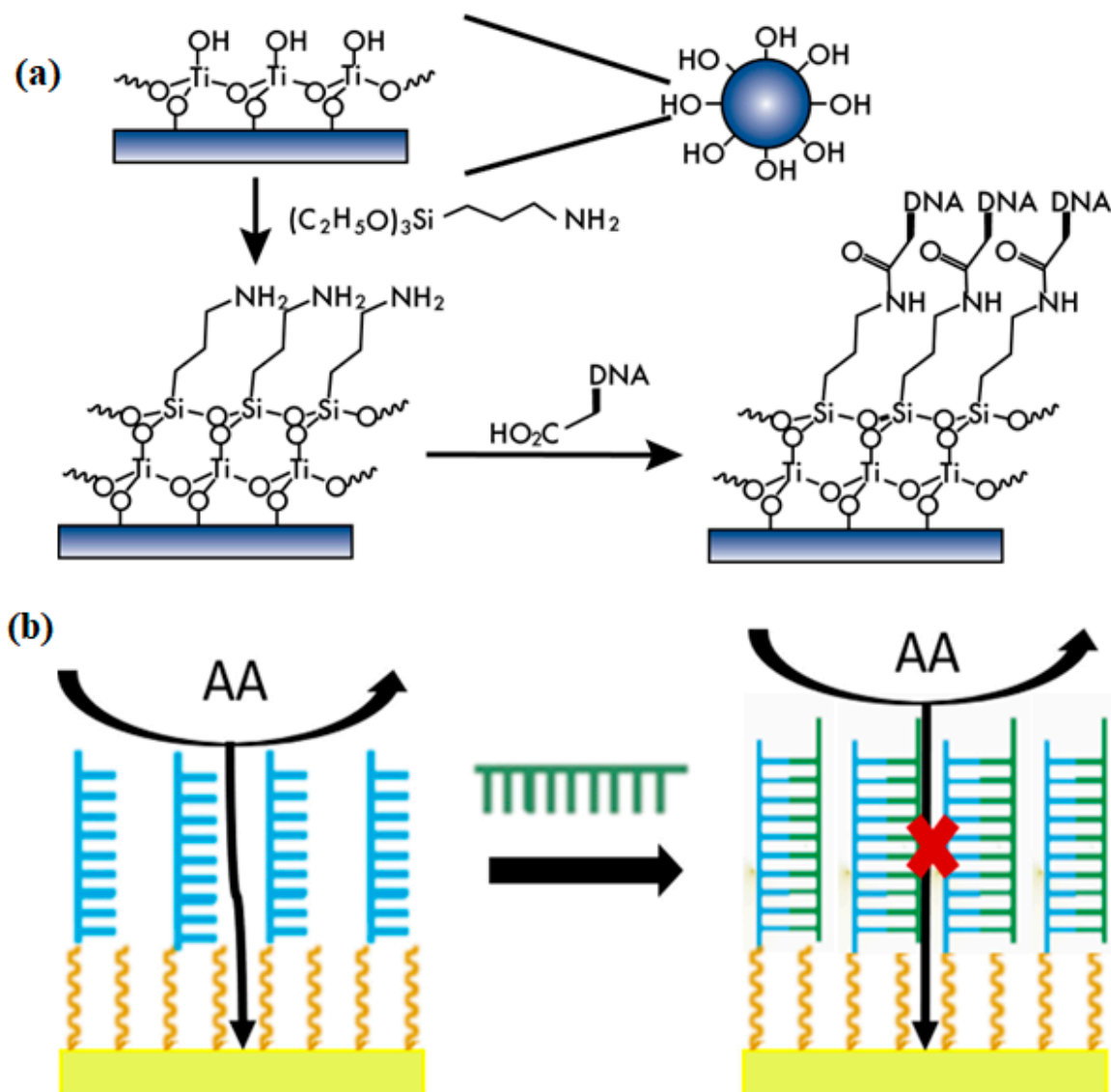


Figure 4. A schematic diagram of the (a) salinization of TiO₂ NPs and the immobilization of DNA on salinized TiO₂ NPs (adapted from [136]); (b) photochemical DNA sensing on the TiO₂ NP surface: the DNA probe (blue) immobilized on the catechol-modified TiO₂ NPs in the presence of ascorbic acid (AA) created a photocurrent which decreased following the target DNA (green) hybridization due to steric hindrance enabling the DNA detection. (Adapted from [126]).

The TiO₂-3,4-dihydroxybenzaldehyde-chitosan photoelectrodes can pave the way for photoelectrochemical DNA detection [137]. TiO₂ nanostructured films are also utilized in developing third-generation biosensors [138,139]. Bacterial cellulose/polypyrrole/TiO₂-Ag (BC/PPy/TiO₂-Ag) film can be utilized to sense and quantify the growth of five harmful bacteria [140]. The electrodes treated with TiO₂/CNT NCs may be utilized in bioanalytical applications such as constructing whole-cell biosensors with improved detection sensitivity [141]. The photoluminescence from TiO₂ NPs can be used as the sensor of Bovine leucosis antibodies because photoluminescence from nanostructured metal oxides has auspicious properties that can be utilized as a sensor for biological compounds [142–144]. The luminous nature of aluminum oxide nanostructures has been used in biosensing applications for a variety of bio-detecting objectives. Al NPs have demonstrated the capacity to detect chemicals in biomolecules [145].

6.2. Metal-Oxide Semiconductors as Biosensors

Numerous metal-oxide semiconductors are utilized as biosensors. ZnO semiconductor nanomaterials can be used as fluorescence-enhancing substrates in biosensing. ZnO can be used to check glucose utilizing an existing general packet radio services (GPRS)/global system for mobile communication (GSM) system. Comparative procedures with different ZnO nanostructure-based systems in the future may invent nanosensors to observe various health parameters [84,146,147].

The complementary–metal-oxide-semiconductor (CMOS) technology is a suitable option that might help answer some of the most important problems in the development of biosensors [148]. Passivation based on atomic layer deposition may be carried out at low temperatures when Al_2O_3 is used. The gadget can be biocompatible. It has a thickness of 50 nm across all its layers. In addition, depending on the requirements of a biosensor array, CMOS-based electrochemical interface circuits may be tailored to provide low noise while maintaining a high degree of sensitivity. This apparatus can evaluate the strength of the cell adhesion as well as the health of the cell. The system is capable of functioning for in vitro cell viability testing for an extended period. In a separate study that made use of the 0.35 μm 2P4M CMOS technology, researchers found that a piezoresistive-type-microcantilever-based system on chip could detect hepatitis B virus DNA constantly without the need to label [141]. In addition, salmonella lens-free CMOS image sensors have been applied to identify bacteria that are transmitted via food. Devices based on CMOS have been developed and used in the creation of retinal prostheses and brain implants. These CMOS-based devices may be used for the stimulation of live cells and have the potential to provide exceptional and flexible use for biological signal detection [141]. The use of CMOS-compatible silicon (Si) nanowires in the configuration of a field-effect transistor has shown significant advantages for continuous biosensing that is level-free and extraordinarily sensitive. An original concept of a split-entryway dielectric modulated metal-oxide-semiconductor field-effect transistor has been presented as a method for label-free electrical detection of biomolecules [149,150]. For example, the cardiac biomarkers CRP and cardiac troponin I (cTnI) were immobilized through the cTnI-specific aptamer and CRP-specific antibodies on Si NWs, which facilitated the rapid detection of biomarkers with high sensitivity. The attachment of both biomarkers on the Si NWs' surface was confirmed by an AFM study. The sensor demonstrated sensitivity towards CRP and cTnI in a wide concentration range from 1 pg/mL to 1 $\mu\text{g/mL}$ [149]. Metal-oxide-semiconductor field-effect transistors have several benefits, including an extended-gate structure and differential-mode activity. These types of biosensors can be utilized with high sensitivity and excellent stability [150]. RuO_2 -based ascorbic acid biosensor demonstrated a sensitivity of 58.43 mV/decade, a linearity of 0.995, a LOD of 1.5 μM , good selectivity for ascorbic acid, and a fast response time of 17 s [150].

6.3. Metal-Oxide-Based Enzyme Biosensor

Enzyme biosensors have been concocted based on immobilization strategies, for example, the adsorption of enzymes through bonding. The enzymes normally utilized for this purpose are oxidoreductases, polyphenol oxidases, peroxidases, and amino oxidases [151]. Though enzyme-linked immunosorbent assays (ELISAs) require a much longer analysis time (~1 h), they have considerably greater sensitivity at low concentrations (~1 pM) [152]. Analytes and biocatalysts mounted on acceptable substrates are required for an enzyme biosensor to work. Nanostructured metal oxides feature biological recognition combined with electrical signal transduction is important in new-generation biosensors. The MONP-based electrode surface's plausibility of direct electron transfer between chemicals can foster unrivaled reagent-less sensitivities [80]. For instance, utilizing gold nanoparticles that are

housed inside tubular nanoclusters of titanium dioxide has allowed for the creation of thiolated enzyme biosensors [153]. Electrochemical Enzyme NP (ENP) biosensors depend on the electrochemical reactions among ENPs and reaction blends. The resultant signs of the electrochemical reactions rely on the sort of transducer utilized which can be estimated as current, voltage, or conductance. An ENP-based biosensor has three electrodes (counter, reference, and working electrode) and these sensors have been utilized to work on the health of individuals, food ventures, and climate monitoring. Among them, the health sector area is the central space of biosensing applications. By utilizing glucose biosensors, the detection of blood glucose levels in diabetic people and an investigation of urea in patients experiencing kidney illnesses can be executed. Additionally, glucose biosensors detect cholesterol, fatty substances, glycerol, and pyruvate levels in heart patients [154]. ZnO NPs are used in developing highly sensitive and selective enzymatic biosensors [155,156]. An enzyme electrode with ZnO nanoparticles and MWCNTs added to it to boost its performance was used to create a novel L-lactate sensor. An enzyme electrode serves as the basis for this sensor's construction [157].

Urine is a complex physiological fluid utilized for many years to recognize certain metabolic disorders, including urinary tract infections, kidney diseases, and diabetes. Urea is the most abundant organic solute in urine, the level of which is utilized for evaluating kidney disorders. The development of a suitable sensor for urea in patients suffering from CKD is crucial to saving their lives. As a terminal disease patients with end-stage renal disease (ESRD) require hemodialysis to remove uremic toxins including urea. The urine nitrogen tests the function of the kidneys. Urinary urea measurement is also utilized as a means of estimation of nitrogen balance in hospitalized patients who are malnourished [158,159]. Several metal oxides and metal/metal-oxide nanocomposites have been studied for the detection of urea. Among them, Ni-based catalysts demonstrated better outcomes in the electrochemical oxidation-based detection of urea. Arian et al. utilized NiO nanomaterials for developing a urease-free simple, highly sensitive, selective, and steady urea sensor for biological samples including blood, urine, and duodenal fluids, and the sensor does not need specific storage conditions [160]. The silver catalyst deposited on ZnO rods/carbon substrate also functions as an enzyme-free urea sensor [161].

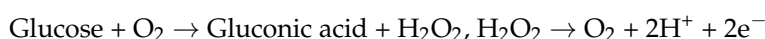
7. Metal-Oxide Biosensor Devices

Metal oxides have assorted chemical and physical properties including bigger active surface area, simpler functionality, high adsorption ability, quick electron-transfer capacity, and tunable bandgaps. They are fundamental for the manufacture of biosensing devices [162]. Among the different metal-oxide NPs, the nano CuO [163], ZnO [164], SnO₂ [165], CeO₂, TiO₂ [80], Fe₃O₄ [166,167], and MgO [168] have biosensor device application. Due to ZnO's high isoelectric point (9.5), it may immobilize elements with a low isoelectric point through electrostatic contact [164–171]. ZnO nanomaterials-based biosensors, for instance, MWCNT/ZnO nanofiber-based biosensors, can be utilized for the detection of malarial parasites [172]. Biosensor innovation has been an expanding interest in nanosized biosensors dependent on ZnO nanomaterials since they have been utilized in the blend of different biosensing molecules. ZnO thin films are incredible for biosensing devices with exceptional sensitivity to manage the cost of a phenomenal stage. These films are created by a flexographic printed procedure, bordering a nanotextured surface during the manufacturing process, and such surface nanostructures have brilliant potential for expanding surface functionalization, which is fundamental for the high sensitivity needed to detect illnesses [173]. As it has been estimated that over 3.4 million individuals die from hypoglycemic and extreme diabetic difficulties, the consistent, consecutive testing of glucose is critical to forestall hypoglycemic and diabetic inconveniences. The efficient glucose

biosensors depend on electrochemical techniques or optical techniques. Most commercial glucose biosensors need disposable glucose test strips, which are costly for successive blood glucose testing. Surface acoustic wave (SAW) biosensors dependent on ZnO films have acquired a lot of consideration since SAW biosensor devices have high sensitivity, reliability, and reusability. SAW devices dependent on ZnO demonstrated superiority and could be incorporated into portable micro-array systems to work with basic and modest electronic components, making them enduring and reasonable for clinical applications [174].

8. Detection of Dangerous Biologics by Biosensor

Biosensors have been utilized for the biological detection of problems like diabetes, cancer, CKD, and allergic responses, that is, different issue-based serum investigations. Examples of uses include recognizing diabetic patients' glucose levels, detecting uremic toxins and infections in the urinary system, detecting HIV/AIDS, and diagnosing cancer [175]. High glucose levels result in diabetes mellitus, and it can be a threat, even though glucose plays an important role in some biochemical processes, such as glycolysis. A high glucose level brings about a metabolic disorder caused by defective pancreatic function. Because enzymes oxidize glucose in a certain way, the great majority of biosensors are geared toward monitoring glucose levels. Since the measurement of glucose levels is vital, this is the primary focus of most biosensors. Glucose biosensors rely only on the enzyme glucose oxidase (GOx). GOx is responsible for the transformation of glucose and oxygen into gluconic acid and H₂O. This transformation enables the glucose biosensors to detect the presence of glucose. Following that, hydrogen peroxide is oxidized electrochemically at a voltage of +500 mV vs. Ag/AgCl.



ZnO nanostructures are utilized in glucose biosensors because their shape has a significant impact on their electrochemical characteristics [176]. The generation of a signal in an ELISA is based on the diffusion of the target component from the sample solution to a solid surface. This test is an excellent example of a heterogeneous biosensor in its typical form. Using a wash step, the detecting signal and the background signal can be separated from one another [177]. To successfully detect SARS-CoV-2, a completely innovative plasmonic-based biosensing device that is also equipped with dual capabilities has been developed [178]. The occurrence of plasmonic phenomena is necessary for the successful operation of this technology. The plasmonic photothermal effect and the localized surface plasmon resonance effect (LSPR) have been combined in the enhanced biosensor to make use of both phenomena. Using lanthanide-doped polystyrene NPs has opened the door to the field of biosensing. Because lanthanides have their unique electronic configuration, lanthanide-doped NPs have the potential to display a broad range of fascinating optical characteristics. The SARS-CoV-2 infection can be diagnosed with the use of biosensors that are based on lanthanide-doped NPs [178]. A fast and sensitive lateral flow immunoassay that utilized Eu-doped polystyrene nanoparticles based on fluorescence technique to detect anti-SARS-CoV-2 IgG in human serum was reported [179]. The method was validated for the identification of anti-SARS-CoV-2 IgG in suspicious cases, which was found convenient for monitoring the progression of COVID-19 and assessing the response of patients to treatment [180]. An electrochemical biosensor that is based on functionalized TiO₂ nanotubes might potentially be employed for the rapid sensing of SARS-CoV-2 [180] (Figure 5). Further, doped with AuNPs, zinc-oxide nanorods can detect Human Papillomavirus-16 in cervical cancer samples [181].

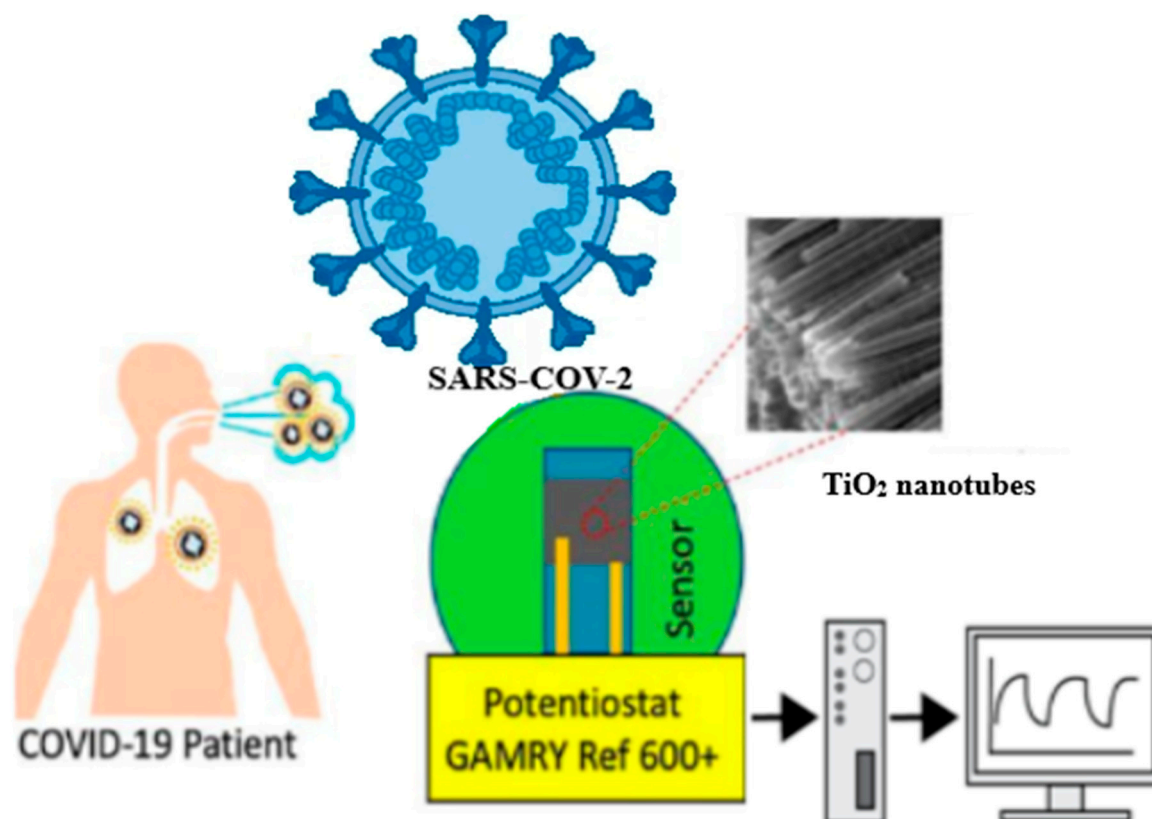


Figure 5. Schematic of co-functionalized TiO₂ nanotube (Co-TNT)-based sensing platform for detecting SARS-CoV-2. (adapted from [180] in modified form).

9. Early Detection of Cancer Using Biosensor

Cancer is an uncontrolled growth of cells brought on by environmental toxins and inherited and acquired genetic and epigenetic mutations. A biomarker is a biological molecule that can be identified in blood, other body fluids, cells, or tissues and acts as an indication of either a normal or abnormal process or a disease or sickness. Cancer biomarkers have the potential to be helpful in the early detection of cancer, the accurate preoperative staging of the illness, the response to chemotherapy, and the development of the disease. The biosensor system is beneficial for early cancer detection and effective therapy, primarily for such cancers that are typically diagnosed at the final stages of the progression of the disease and demonstrate poor sensitivity to therapy, which ultimately results in an improvement in patient quality of life and the prolonged survival [182]. Different types of electrochemical biosensors utilizing various support materials such as carbon allotropes, polymers, metal nanoparticles, and nanocomposites, biomolecules such as immunoglobulins, nucleic acids, and hormones are useful in cancer diagnosis, particularly for point-of-care testing (POCT) [183]. Recently, a tapered optical fiber (TOF) plasmonic biosensor was developed and employed for the sensitive detection of a panel of microRNAs (miRNAs) in human serum taken from people with and without prostate cancer (PCa). Since multianalyte detection reduces the number of false positives and negatives and provides a solid basis for early PCa diagnosis, the oncogenic and tumor suppressor miRNAs let-7a, let-7c, miR-200b, miR-141, and miR-21 were evaluated as predictive cancer biomarkers. Further, multianalyte monitoring reduces false-positive and false-negative rates and offers the opportunity for early PCa diagnosis [183].

The biosensing platform has metallic gold triangular nano prisms (AuTNPs) coated on the TOF to stimulate surface plasmon waves in the supporting metallic layer and boost the evanescent mode of the fiber surface. Without RNA extraction or sample amplifi-

cation, this sensitive TOF plasmonic biosensor, as a point-of-care cancer diagnostic tool, enabled the identification of the panel of miRNAs in the serum of the patients. With a detection limit between 179 and 580 aM and good selectivity, the TOF plasmonic biosensor could detect miRNAs in human serum. With a p-value of less than 0.0001, statistical analyses were conducted to distinguish malignant from noncancerous samples. This high-throughput TOF plasmonic biosensor has the potential to advance and expand POCT for cancer diagnoses [184].

Cancer and genetics are interlinked. So, DNA analysis is most important in cancer treatment and diagnosis. DNA biosensors have been recognized as a screening tool that can be used for the bioanalysis of environmental pollution studies as well as DNA-drug reactions. The concept of testing at the point of care has emerged as the new top priority for biosensor applications. It is now feasible to dramatically enhance the delivery of health services and healthcare due to POCT [185]. The diagnosis of cancer in clinical medicine is now mostly dependent on imaging tools as well as the morphological study of diseased cells or tissues. Particularly, 2D nanomaterials have found great uses in the construction of electrochemical biosensing platforms, which have enabled the very sensitive detection of cancer markers present in extremely low concentrations in relatively small amounts of a variety of clinical samples [186]. Two-dimensional graphene nanomaterials functionalized with Fe_3O_4 , MoO_3 , Si/SiO_2 , Cu , Au , Pt , etc., have shown promise in electrochemical biosensing systems to screen and diagnose different types of cancer both *in vitro* and *in vivo*. The H_2O_2 sensors based on a graphene nano-sheet decorated with Pt , Au , and CuS have been fruitfully utilized for monitoring H_2O_2 liberated from different cancer cells, as well as quantifying H_2O_2 levels in human serum and urine samples [186]. Further, a graphene-based ternary nanocomposite such as an rGO nanocomposite decorated with Au , Pt , and Fe_3O_4 nanoparticles was employed to fabricate a sensitive electrochemical biosensor for the detection of H_2O_2 released from cells during redox hemostasis distraction by ascorbic acid, including human cervical cell lines (HeLa), human primary glioblastoma cell lines (U87), human hepatocellular carcinoma cell lines (HepG2), and human embryo liver cell lines (L02). The study provided crucial information on the intracellular tumor microenvironment during the tumor development process. The nanostructure microelectrode based on Au NPs, MnO_2 nanowires, and a graphene nanosheet-coated carbon-fiber electrode demonstrated excellent sensitivity, reproducibility, stability, and selectivity, making it ultrasensitive and specific for real-time tracking of the secretion of H_2O_2 from human HeLa cells and human normal mammary epithelial cells, HBL 100 [186].

Prostate-specific antigen (PSA) was one of the first tumor biomarkers used for the identification and monitoring of prostate cancer. Smith discovered that 30% of males with PSA levels between 4.1 and 9.9 mg/mL had prostate cancer. A PSA result that is unusually high may suggest the existence of benign prostatic hyperplasia, prostatitis, or a benign prostate tumor. Abnormally high levels of cancer antigen (CA) 125 have been linked not just to ovarian cancer but also to uterine, cervical, pancreas, liver, colon, breast, lung, and digestive cancers. The most frequent kind of cancer related to CA 125 levels is ovarian cancer. As a crucial biomarker, the CA 15-3 levels of breast cancer patients are measured. Currently, the levels of CA 15-3 are included in the development of therapy protocols. Other parameters, such as tumor size, malignancy stage, and unfavorable risk factors (such as HER-2 status and ER/PR status), are also taken into consideration. In addition to generating an increase in CA 15-3 levels, endometriosis, pelvic inflammatory disease, hepatitis, pregnancy, and breastfeeding can all be contributory factors. Among the many types of cancer biomarkers, cancer-testis (CT) antigens stand out. The presence of CT autoantibodies in serum, which is far more accessible than tissue biopsies, is a benefit of CT autoantibodies as cancer biomarkers. Therefore, they could be especially useful for

forecasting the onset and/or development of cancer [182]. An early diagnosis, which makes use of biomarkers that are particular to prostate cancer, has the potential to significantly increase the prostate cancer survival rate while simultaneously reducing the total costs of therapy. miRNAs have attracted a lot of interest as potential biomarkers due to the critical role that they play in several physiological and pathological processes, one of which is the development of cancer. Functional research has shown that abnormal expression of miRNAs may have a direct impact on the progression of prostate cancer. This is because of aberrant miRNA expression targets components that oversee governing processes such as the development of the cell cycle, apoptosis, DNA repair, differentiation, androgen signaling, angiogenesis, hypoxia, and chromatin remodeling. It is typical for patients with prostate cancer (PCa) to have an elevated level of oncogenic miRNAs. This level of oncogenic miRNAs contributes to the progression of cancer by inhibiting the activity of tumor suppressor genes (i.e., TP53, PTEN). Similarly, tumor suppressor miRNAs are found in the prostate of cancer patients. These miRNAs prevent the formation of malignant tumors and govern the differentiation or death of cancer cells by focusing on oncogenic factors, which allows them to do both simultaneously [182,187].

The introduction of label-free chemical imaging techniques in biological samples has sparked a significant amount of interest in mass spectrometry imaging, which has successfully garnered a significant amount of this attention [177]. Antibody arrays, in which antibodies are organized in a two-dimensional pattern on a solid substrate, are one use of this ground-breaking method. One possible use for this technique is antibody arrays. The capacity of the antigens to bind to certain antibodies at specified sites allows for the detection of a variety of different antigens using antibody arrays. Automated multi-analyte analysis is feasible with the use of these array biosensors, microfluidics technology, and a detecting element. The use of integrated biosensor chips may enable a thorough study of a challenging biospecimen, such as blood or other bodily fluids [188]. Zinc-oxide and iron-oxide (Fe_2O_3) films are innovative solid support for DNA microarrays and may be effectively utilized for cancer diagnosis [189]. GeO_2 -, TiO_2 -, Al_2O_3 -, and B_2O_3 -doped fused silica-based fluorescent biosensors may be utilized for the detection of cancer biomarkers [190]. A peptide-based PEC biosensor was constructed based on the CdTe/ TiO_2 -sensitized structure as the electrode and CuS nanocrystals as a signal amplifier to detect PSA with good specificity, stability, and reproducibility in a linear range from 0.005 to 20 ng/mL. The sensor was constructed based on a reaction that the PSA specifically cleaves a specific amino acid sequence [191,192]. Neuron-specific enolase (NSE) is a tumor biomarker with expression in non-small cell lung cancer. A 3D-hyperbranched TiO_2 nanorod array was fabricated and utilized to construct a dopamine-sensitized PEC biosensor for the detection of NSE. In this sensor, dopamine was used as a sensitizer and combined with a TiO_2 nanorod array to achieve signal amplification. The biosensor demonstrated an excellent linear relationship range from 0.1 ng/mL to 1000 ng/mL, with a detection limit of 0.05 ng/mL for NSE detection [193]. A PEC immunosensor for NSE detection based on a Z-scheme $\text{WO}_3/\text{NiCo}_2\text{O}_4/\text{Au}$ nanoarray p-n heterojunction utilized the LSPR effect of Au to convert thermions into a photocurrent to achieve signal amplification. NiCo_2O_4 with good electrical conductivity and $\text{WO}_3/\text{NiCo}_2\text{O}_4$ with a large specific surface area and a large number of active centers for the loading of polyamidoamine films were utilized in biosensor fabrication. The constructed PEC immunosensor for NSE detection was used in the range of 0.1 pg/mL to 50 ng/mL. The logarithmic value of NSE concentration showed a linear relationship with the photocurrent intensity with a LOD of 0.07 pg/mL [194]. TP53 is one of the most muted genes in cancer. TP53 is an important tumor marker for colon cancer. A sensitive fluorescent biosensor based on DNA-functionalized Fe_3O_4 NPs was fabricated for the detection of TP. The consensus DNA was immobilized on animated

dextran-modified Fe₃O₄ NPs and tagged by Cy-5 to generate a fluorescent signal. The interaction between DNA and TP53 protein led to a decrease in fluorescent emission, enabling the detection of the TP53 tumor marker. The DNA-functionalized Fe₃O₄ NP sensor for TP53 detection had a detection limit of 8 pM and a linear range of detection from 50 pM to 2 nM [195]. Carcinoembryonic antigen (CEA) is a tumor marker for gastrointestinal tumors. Two-dimensional TiO₂ nanosheets were modified with carboxylated graphite carbon nitride (g-C₃N₄) with a strong photocurrent. The antibody of CEA was bound to the nanosheets, and the specific binding of CEA and its antibody decreased in the photocurrent allowed for the detection of CEA [196]. Human epidermal growth factor receptor 2 (HER2) is a tumor biomarker for breast cancer. HER2-positive breast cancer has a high degree of malignancy and accounts for 20–30% of molecular types of breast cancers. Magnetic Fe₃O₄ nanospheres, spherical and uniform in shape, were modified with anti-HER2 antibodies to proficiently capture HER2 in serum samples. The signal amplification was performed with ascorbate oxidase-modified Co₃O₄ NPs and HER2 aptamers. The detection of the HER2 was based on the reduction in photocurrent intensity. The selectivity and specificity of the HER2 sensor were detected using human IgG, CEA, BACE1, p53, and human IgM, which confirmed its good specificity and selectivity. The linear range was 1 pg/mL to 1 ng/mL and the LOD was 0.026 pg/mL for the HER2 sensor [197].

10. Enzyme-Less Metal-Oxide Biosensors for Biomarker and Biomolecule Detection

The recent developments in nanomaterial research have facilitated a huge breakthrough in smart, portable, and electronic devices. Their high-end features like excellent sensitivity, portability, fast response, flexibility, validity, and stability have drawn significant attention from consumers, promoting their use in day-to-day life in the biomedical and healthcare sectors. As a result, these enzyme-less portable sensor devices need to be further developed by supplying low-dimensional binary or ternary nanostructure material for continuous use. To boost the usage demand in everyday life, enzyme-less nanomaterial sensors fabricated from nanomaterials, conductive polymers, and other available sources have received remarkable attention to meet the demand in the upcoming decades for portable biomedical devices due to their stability, reusability, and long-term applicability. Therefore, researchers have been interested in integrating different functional electro-active low-dimensional doped nanostructure materials and their NCs with green sources for portable use in biomedical and healthcare sectors on broad scales. In this era of modern electrochemical research, enzyme-less sensors have shown remarkable accomplishment because of their wide operation ranges, elevated sensitivity and large-linear dynamic ranges, long-term stability, reproducibility, fast response, validity, and uses in conventional devices and tools. Different selective and sensitive enzyme-less biosensors were developed with various nanostructures or NC materials [198–200]. The enzyme-less γ -amino-butyric acid sensor has been introduced with low-dimensional copper-oxide NPs by an electrochemical approach. The sensor exhibited good sensitivity, a large linear dynamic range, the lowest limit of detection (11.70 pM), a good limit of quantification (39.0 pM), and robustness. The impedance impacts were assessed by the I-V strategy with the proposed sensor (GCE/naion/CuO NPs) for the γ -amino-butyric acid sensor [201]. A CuO NC sensor exhibited good electrochemical performances. This sensor probe has been validated with biological samples, for instance, human serum, mouse serum, and rabbit serum, with acceptable and satisfactory results [191]. A low-dimensional doped silver oxide nanorod was synthesized wet-chemically and applied for enzyme-less choline detection by an electrochemical approach [202,203]. Further, the CdO/SnO₂/V₂O₅ micro-sheet sensor probe was validated with real biological samples. This study introduced a noble approach to

detect unsafe biological matter with CdO/SnO₂/V₂O₅ micro-sheets/nafion/GCE sensor probes [204].

Creatine (CA) is produced in the liver and kidney in humans and distributed through the blood circulation in the body. The CA is then carried out to tissues with high energy demands in the body, such as the brain and skeletal muscle. CA is also found in meat and vegetables which are common in the human food chain. CA has a vital role in energy production and control of the pH of the buffer system in the living tissues. As a result, the continuous delivery of CA is essential either through biosynthesis or by food in the human body [159,205,206]. A shortage of CA may result in several neurological symptoms such as autism, extrapyramidal syndrome, hypotonia, auto-mutilating behavior, delays in speech acquisition, and neurodevelopmental disorders [207–209]. Creatinine is a breakdown product of CA phosphate from muscle and protein metabolism. In normal healthy people, creatinine is excreted from the body through the kidney. Creatinine is released into the circulation and almost exclusively excreted in urine. Creatinine is easily filtered by the glomerulus, and unlike urea, it is not reabsorbed or affected by urine flow rate. If the kidney function is not healthy, creatinine levels in the body will increase. In the case of a CKD patient, excess creatinine is accumulated in the body as a uremic toxin, because the kidney loses its normal filtration activity due to its failure to function normally.

Considering the pathophysiological aspects of CA in humans, it is crucial to develop reliable and effective sensors for CA in biological systems. The normal serum CA is in the range of 0.6 to 1.2 mg/dL or 53 to 106 μmol/L for adult males and slightly lower (~10%) in adult females [210]. CA is produced in the body at a virtually constant rate and its concentration in blood changes a little in healthy people. However, it may be elevated in some pathological conditions such as metabolic disorders, including CKD and cancer. Like proteinuria, a high creatine level is a sign of a likely health problem, rather than a problem itself. If the creatine level increases because of kidney issues, one may experience related indications. The derivative CA riboside is a significant metabolite of cancer metabolism. It is used as a urinary biomarker of lung and liver cancer risk and prognosis. Some of the existing approaches generally utilized for the quantification of CA in human fluids such as urine and blood include calorimetry, spectrophotometry, and fluorometry [211–213]. These conventional strategies for CA quantification face some difficulties, such as heavy and expensive instruments, the time-consuming process, the costly reagents, and the lack of portability. Figure 6 represents the metabolic biomarker detection process with GCE decorated with porous nano-formulated CMNO materials, such as the detection of CA with GCE decorated with porous nano-CMNO materials. The higher sensitivity and lower detection limit, stability, fast response time, large linear dynamic range (0.1 nM–0.1 mM), repeatability, and validity were significantly determined with this electrode assembly in the phosphate buffer phase. This research method is an effective enzyme-less sensor probe for metabolic biomarkers for kidney disease, cancer, etc. [205].

The higher level of uric acid is very unsafe and toxic to human health, and it is necessary to develop an enzyme-less biosensor probe for detection [214]. The association of hyperuricemia with CKD is attributed to the retention of serum uric acid that occurs as the glomerular filtration rate falls. Uric acid may have several roles in kidney disease. Uric acid induces chemokines in tubular cells and can tempt intrarenal inflammation. Diabetic patients may develop elevated serum uric acid, and a reduction in uric acid level could lower kidney disease [215]. Cyclosporine may raise the uric acid level, and the renal disease induced by cyclosporine could be worsened by increasing the uric acid level and improved by reducing it [216,217]. A method has been developed utilizing CuO nanomaterials to detect uric acid [218,219]. Large linear dynamic range, stability, sensitivity, reproducibility,

response time, lower limit of detection, and long-time stability were observed and further validated in the real sample.

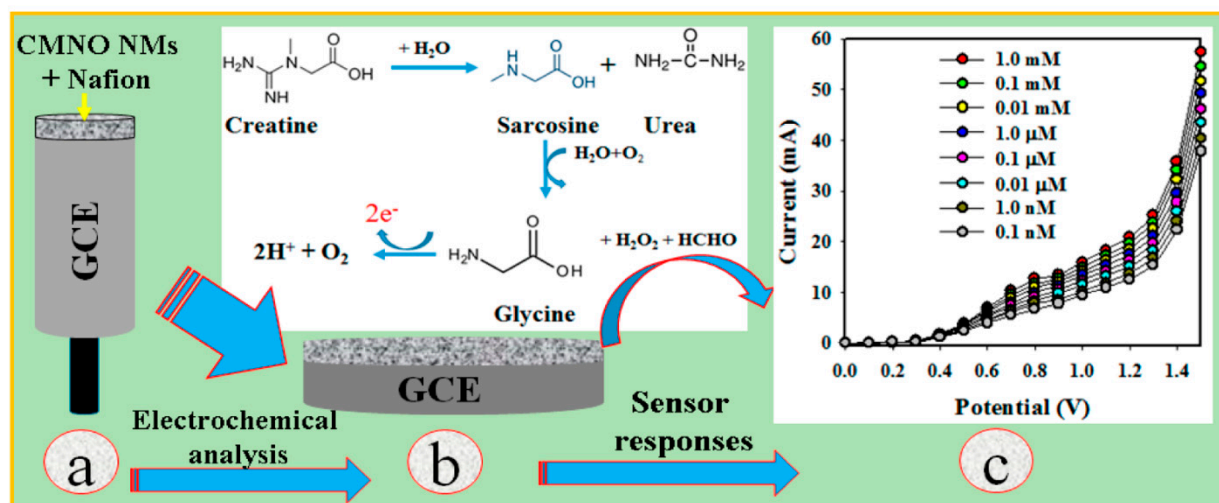


Figure 6. Schematic representation of creatine biomarker detection with CMNO-decorated GCE for the creatine. (a) Modification of glassy carbon electrode (GCE) with CMNO NMs, (b) electrochemical oxidation of CA on CMNO NMs/GCE, and (c) responses recorded in electrometer. (adapted from [205]).

A metal-oxide-based heterojunction thin-film transistor (HJ-TFT) using In_2O_3/ZnO was developed for the label-free fast detection of uric and vitamin D3 in PBS and human saliva. The HJ-TFT used a solution-processed In_2O_3/ZnO channel that was functionalized with a uricase enzyme and vitamin D3 antibody for the selective detection of uric acid and vitamin D3 [220]. The ultra-thin tri-channel system facilitates enhanced coupling between the electron transport along the buried In_2O_3/ZnO interface and the electrostatic perturbations caused by the interactions between the surface-immobilized receptors and target analytes. HJ-TFT-based microarray for the noninvasive detection of uric and vitamin D3 in human saliva demonstrated steady performance under physiologically relevant conditions. The sensor system was able to detect uric acid at a concentration range of 500 nM to 1000 μ M, and 100 pM to 120 nM vitamin D3 within 60 s, respectively. The LOD for uric acid was \sim 152 nM and that for vitamin D3 was \sim 7 pM. HJ-TFT microarray biosensor system exhibited specific detection of uric acid and vitamin D3 by the selective functionalization of the individual transistors with uricase enzyme and vitamin D3 antibody [220].

$Co_3O_4-SnO_2$ NPs can be utilized for the detection of selective L-glutathione [221]. Non-enzymatic glucose detection is possible by utilizing AuNP-anchored poly-aniline blue (PAB) NCs on a glass substrate covered with fluorine-doped tin oxide (FTO), AuNP/PAB/FTO. The PAB has been applied to the FTO electrode using cyclic voltammetric sweeping to obtain a high level of surface coverage. On the PAB/FTO electrode, AuNPs are then deposited using the seed-assisted growth method. When glucose in its native state has been oxidized, the NCs demonstrated potent electrocatalytic activity. Two linear responses with sensitivities of $1.30 \mu A cm^{-2} \mu M^{-1}$ and $0.12 \mu A cm^{-2} \mu M^{-1}$ have been identified in the concentration ranges of 2–50 μ M and 50–250 μ M. The difference between these concentrations was 250 μ M. The most sensitive level of this sensor can detect things up to 0.40 μ m away. Due to the sensor's high repeatability, long-term stability, and excellent glucose recovery in real samples with little interference, it has been used several times without losing precision [222]. Cu-NPs have been effectively coated on the side wall of MWCNTs using a polyelectrolyte as a template for a simple and effective in situ process. Due to the presence of polyelectrolytes in these materials, NCs may undergo fast changes in GCE. This

has occurred due to the presence of polyelectrolytes in the environment. Utilizing CV and chronoamperometry as the principal techniques, the glucose oxidation activity of modified electrodes has been investigated. Under alkaline conditions, the NCs demonstrated potent non-enzymatic electrocatalytic reactions to glucose. As a result, using NCs, researchers may investigate and build glucose sensors that do not depend on enzymes [223]. To study rabbit serum, orange juice, and urine, the ZnO-CuO sensor probe has been developed and found acceptable with satisfactory results for acetylcholine and ascorbic acid sensing, which demonstrated sensitivity ($317.0 \text{ pA}\mu\text{M}^{-1}\text{cm}^{-2}$ and $94.94 \text{ pA}\mu\text{M}^{-1}\text{cm}^{-2}$), stability, lowest detection limit (14.7 pM and 12.0 pM), good quantification limit (490.0 mM and 367.0 mM), linearity ($R^2 = 0.9049$ and 0.9201), large linear dynamic ranges, repeatability, and short response times, in large concentration ranges (100.0 pM–100.0 mM). For the safety of biomedical and healthcare industries in general, this method introduces a novel approach to simultaneously detect acetylcholine and ascorbic acid using binary doped nanostructure material via an electrochemical approach. Another oxidative stress indicator is hydrogen peroxide, which may be a symptom of terminal illnesses including cancer, aging, and brain damage from trauma as well as ischemia/reperfusion problems and memory loss. Due to its medicinal significance and status as a major agent, a sensitive and accurate method of determining its concentration is needed. For the hydrogen peroxide detection with flower-flake La_2ZnO_4 NCs material, researchers have introduced a non-enzymatic sensing matrix by an electrochemical approach in room conditions, where the target H_2O_2 analyte has been detected selectively with higher sensitivity [224].

The nitrite (NO_2^-) analyte has been implicated in many health complications such as cancer and oxygen deficiency in blood when it exceeds the limit. The graphene oxide–polyaniline–Au NP (GO-PANI-AuNP) nanomaterial has displayed an enhanced electrochemical conductance as well as electro-catalytic activity towards the target nitrite analyte compared to other sensors. Good sensor analytical parameters have been obtained with good selectivity of 0.5 micrometer to 0.24 mm [225]. A non-enzymatic sensor composed of AuNPs/PANI/SnO₂ NCs has been developed to enhance the electrochemical detection of nitrite. These NCs were created to combine the beneficial properties of MONPs, conducting polymers, and noble metals. Several spherical AuNPs were dispersed throughout the fibrous PANI-SnO₂ surface. The sensor responded effectively to NO_2^- detection. Additionally, this sensor exhibited superior selectivity, stability, and repeatability. Au/PANI/SnO₂ can serve as a novel sensor for the non-enzymatic sensing of NO_2^- [226]. Cu₂S nanorods on 3D copper foam (Cu₂S NRs@Cu foam) were fabricated in situ at reasonable costs and with little effort. Cu₂S NRs@Cu foam has the potential to be used as a source for the non-enzymatic detection of glucose and H_2O_2 in biological samples. This biosensor has shown high sensitivity and a low detection limit for the electrocatalytic oxidation of glucose. When presented to H_2O_2 , this nonenzymatic sensor exhibited an outstanding response, for instance, high sensitivity ($1.686 \text{ mA mM}^{-1} \text{ cm}^{-2}$) and low detection limit (0.2 μM). It has offered a method that is both effective and promising for the development of non-enzymatic glucose and H_2O_2 sensors and may be used in real-world applications [227]. Malathion (MLT) is a kind of organophosphorus pesticide, and it has very high toxicity. Electrochemical platforms for the rapid, simple, cost-effective, and sensitive testing of pesticides remain a challenge. The AuNP-CS-IL/PGE (pencil graphite electrodes) NCs were evaluated for their prospective use as a sensing matrix in the non-enzymatic electrochemical detection of malathion. This has been accomplished by utilizing cyclic voltammetry and square wave voltammetry to conduct measurements. The findings showed that electrodes modified with AuNP-CS-IL can be used to perform a simple, quick, highly sensitive, and cost-effective detection of MLT [228]. It has been shown that enzyme-free glucose detection can be carried out using Fe_3O_4 nanotubes (NTs) on FTO as a nanoelectrode. The Fe_3O_4 NT array's me-

mechanical stability has made it a feasible material for electrochemical sensing. When utilized for amperometric glucose detection, it has shown a powerful electrocatalytic reaction with a detection limit of 0.1 μM , rapid response, and excellent sensitivity. The electrochemical detection potential of this array electrode is high, and it can be employed with a wide range of analytes [229]. Using a standard wet chemical technique, the copper foil has been used as the substrate for the deposition of uniform, petal-like CuO nanostructures at room temperature. Their electrochemical performance has been assessed using cyclic voltammetry, amperometry, and electrochemical impedance spectroscopy. CuO films have been proven to be active electrode materials for the non-enzymatic amperometric detection of H_2O_2 with a lower detection limit and higher sensitivity. This electrode is an especially sensitive and reliable device for non-enzymatic electrochemical detection of H_2O_2 [230].

The hybridization chain reaction (HCR) and dsDNA-templated copper NPs have been used to generate a label-free and non-enzymatically amplified fluorescent method for DNA detection. Without the need for enzymes, this approach can identify DNA. The biotin and streptavidin interaction has been used to connect biotinylated capture DNA probes to streptavidin-modified beads. The target DNA then hybridized with the capture DNA probes to produce sticky DNA. The sticky end stimulated the HCR process and dsDNA polymerization despite the presence of two hairpin probes at the same time. CuNPs with high fluorescence properties were created utilizing dsDNA polymers as a template, resulting in a non-enzymatic signal response. The fluorescence detection method, on the other hand, is reliant on HCR activation by the target DNA. In biological and medical applications, the suggested notions and approaches in this research hold a lot of potential for quantitative DNA identification [231].

11. Metal-Oxide Biosensors in Healthcare and Environmental Protection

Metal-oxide-based biosensors have significant applications in the healthcare and environmental sectors. Biosensors that can detect nitrogenous substances like urea are critical for reducing economically motivated adulteration (EMA) in the food and dairy industries. US-FDA has categorized urea among chemicals most likely to be used in protein adulteration. In milk, urea is illegally added to increase solid nonfat (SNF) value and nitrogen content to mislead the testing result of protein content. Such an adulteration of milk with cheap toxic chemicals like urea poses a serious health hazard. The acceptable range of urea in milk is 70 mg/dL. Above this limit, urea has fatal effects on human health, particularly in children's. Excess urea in milk can cause indigestion, renal failure, urinary tract obstruction, gastrointestinal bleeding, and cancer [232]. An aptasensor utilizing gold NPs (Au NPs) was developed to detect urea in milk [232]. Here, DNA aptamer interaction with urea was evaluated by affinity, melting curve analysis, CD, and truncation tests. A user-friendly, "non-enzymatic" aptasensor with dual readouts was developed that interpreted intrinsic fluorescence variations and color changes produced by aptamer-urea binding simultaneously. This sensor has high selectivity in the detection of urea. The response signals increased in proportion to the amount of urea adulteration in the milk. The detection limit for urea adulteration in milk was 20 mM to 150 mM [232].

To increase food and agricultural production, it is necessary to utilize pesticides to protect plants. However, this approach poses pesticide poisoning and also increases environmental hazards. An urgent development of pesticide detection technologies to save the environment is thus crucial. There have been many efforts to develop technologies for the development of sensors for different pesticides [233]. Pesticides are frequently utilized in crop production; however, they may substantially affect both the environment and human health. Therefore, an effective biosensor for pesticide detection must control pesticide utilization and safely enhance crop production.

Metal-oxide-based biosensors have shown great promise in healthcare applications, as electrochemical biosensors based on NiO were utilized in the sensitive detection of 4-acetaminophen, a NiCo₂O₄ biosensor was applied for the detection of glucose and lactic acid, and a NiCoZnO biosensor was utilized to detect dopamine in biofluids [234].

Therefore, metal-oxide-based biosensors facilitate the immobilization of DNA probes and antibodies, enabling the specific detection of nucleic acids and proteins, which has applications in the diagnosis of genetic, infectious diseases, and cancer. Metal-oxide biosensors are useful for recognizing uric acid, dopamine, and lactates and identification of pathogens and hormones. Biosensors are also effective in the detection of pesticides and other environmental toxins [235,236].

12. Conclusions

A variety of biosensor types based on promising transducing mechanisms are being investigated, including electrochemical, thermal, optical, and piezoelectric biosensors. Metal-oxide NPs have been applied for quick and exact biomolecule detection. MONPs are auspicious in sensing pathogens, dangerous biologics, and other important species of the human body. There have been numerous progressions in material manufacturing methodologies, enzyme/protein designs, and immobilization/conjugation approaches, which have advanced novel nanoparticles with further developed functionality. Uses of metal/metal-oxide biosensors include recognizing diabetic patients' glucose levels, detecting uremic toxins and infections in the urinary system, detecting HIV/AIDS, and diagnosing cancer. ZnO-based electrochemical biosensors have been used for the detection of a variety of analytes such as uric acid, glucose, cholesterol, dopamine, and DNA. Metal-oxide-based optical biosensors are promising in identifying *E. coli* and *Listeria monocytis*, CRP, cTnI, Tau proteins, DNA, and other biomolecules. An electrochemical biosensor based on functionalized TiO₂ can potentially be employed for the rapid detection of SARS-CoV-19. Zinc-oxide nanorods doped with gold NPs can detect Human Papillomavirus-16 in cervical cancer samples. Piezoelectric biosensors are excellent sensors for lymphocytes and immunoglobulins such as SiO₂/ZnO nanowires modified with AuNPs, which can be utilized for detecting IgG, and Au/PANI-NF sensors applied for monitoring the T cell activation. The anti-CD antibody molecule was immobilized onto the composite to observe the activation by studying the expression of CD69, CD25, and CD. Research in the state-of-the-art field of biosensing with biofunctionalized multifunctional nanomaterials, and the advancement of practical biochips utilizing nanoscale sensing material, are very promising and prospective. Biosensing is an auspicious approach in the biomedical arena, particularly in cancer, CKD, AD, and the detection of and protection from other diseases.

13. Current Challenges and Future Perspectives

Even though biosensors can be installed in a certain setting, it is far more challenging to use them in biological matrices like body fluids. This is because biological matrices are more complex. Research on biosensor application, diagnosis, and follow-up analytical equipment may be distinguished from research on biosensors [237]. The presence of interference signals brought on by interferences is a common problem in biosensing. This problem arises when a sensor is in persistent contact with biofluids, for example, oxidizable acids, and bases of larger and lower molecular weight. These have the potential to cause interference. In addition to this, it is quite likely that metabolites derived from pharmaceuticals will be found in the fluids of the body (e.g., acetaminophen). Allosterically, interfering proteins with a high molecular weight adsorb on the surface of the transducer. This is known as an allosteric interaction. Because of this methodology, the chemicals, which are often found in very trace levels, are not detected even if they are present there [238].

The biological medium contains a broad variety of substances, any one of which can encourage the growth of biofouling or cause enzymes to become inactive. In addition to proteins, these molecules can include water-soluble small molecules (such as carbohydrates), as well as hydrophobic substances (e.g., lipids). Electrode passivation and biofouling develop from any contact with these chemicals. Polyurethanes with phospholipid-polar polymers, 2-Methacryloyloxyethyl phosphorylcholine, polyvinyl alcohol hydrogels, hyaluronic acid (HA), and phosphorylcholine are the components that make up these membrane coverings. Phosphorylcholine, HA, and humic acids are some of the other components that may be used to coat membranes. These membranes diminish protein adsorption, which in turn allows target analytes to reach the surface of the biosensor where they can be detected. This helps to lessen the influence of biological fluids on biosensors. Protein fragments with a low molecular weight as well as large, charged cell deposits have a lower level of resistance to these approaches [237]. Enzymes can be stimulated or stifled by the presence of cations in biological fluids, whether they are monovalent or divalent. Cation effects on enzymes can be influenced by any one of these effects. The structure of cations determines whether they are monovalent or divalent. This opens the door for the use of allosteric effectors, which are not involved in the enzymatic activity or conformational requirements required for catalytic performance, but have a function. Catalysis is not influenced by allosteric effectors in any manner, shape, or form, and an effector that does not participate in the catalytic process is referred to as an “allosteric effector.” There is a chance that one of these occurrences will ensue at some time. The size of the catalytic region and charge are regarded to be the two most important factors when selecting whether a metal ion can block an enzyme [239]. Monovalent cation interactions with enzymes are critical in some circumstances, such as when K^+ and Na^+ protect glucose oxidase against heat denaturation [240]. Proteins and lipids may sometimes adsorb onto an electrode in a non-specific manner, which can result in the electrode being passivated. Polymeric films, in addition to other films, can circumvent the passivation process. On the other hand, this would result in a delay in the responses that are provided. To reduce the amount of fouling that can occur on electrodes, such as that which is caused by the oxidation of NADH, carbon nanotubes have also been used [241,242].

The development of nanophotonic devices, which can control light in quantities less than a wavelength and boost the number of interactions between light and matter, has cleared the way for new biosensing opportunities. The limits of existing bioanalytical technologies in terms of sensitivity, throughput, convenience of use, and downsizing have inspired the development of a great deal of nanophotonic biosensors in recent years [243]. When dealing with biological material, it is best to use disposable biosensor chips, since they prevent the spread of infection and eliminate the need for labor-intensive cleaning processes. In this context, the most workable integration solutions are those that support both single-use cartridges and independent readers. For example, the nanophotonic biochip can be put in a disposable cartridge that is kept separate from the light source and detector. These types of disposable cartridges can be customized to function as consumables for detecting a variety of analytes using the same reader. This scenario can cut reader costs by permitting the use of off-the-shelf optoelectronic components. It also has additional advantages over multiuse biosensor designs, which generally degrade sensor efficacy and boost ultimate cost due to approaches for surface functionalization renewal. However, to manufacture affordable cartridges that are intended for a single use, it is necessary for this technique to need monitoring regarding the cost of biomaterials [244]. It is becoming more common to use nanophotonic biosensors in conjunction with smartphones. This is because the light sources, cameras, image recognition capabilities, and connections offered by smartphones may help to reduce costs and make it possible to disseminate

information on a large scale [245–247]. They would be used to gather data from patient samples through wireless transmission, and then custom software would be utilized to analyze the results of that data collection. It is true that single-use biosensors have a smaller physical footprint and are simpler to carry. Still, the manufacturing and packaging operations related to their various device layers contribute to an increase in the cost of these biosensors. Because of the versatility of these methods in producing a wide variety of nanostructures, engineers have mostly relied on electron-beam or focused-ion-beam lithography to create nanophotonic biochips. Because the currently used techniques for serial patterning have poor throughput and a high cost, it is necessary to create alternative, more cost-effective manufacturing methods.

Gold and silver are incompatible with front-end CMOS processing. It is projected that low-cost, large-scale, top-down lithography techniques such as nanoimprinting, nano stencils, interference lithography, and deep and severe UV lithography can gain popularity as alternatives to the manufacturing methods that are now in use [248]. As the choice and arrangement of nanomaterials are basic for quick and exact biomolecule detection, the constant progressions in material manufacture methodologies, enzyme/protein designing, and immobilization/conjugation procedures will keep yielding novel nanoparticles with further developed functionality. Research in the field of cutting-edge biosensing with biofunctionalized multifunctional nanomaterials, and the advancement of practical biochip plans utilizing nanoscale sensing materials can additionally prepare for nano-biosensing stages. An imaging blend of recently emerging fabricating methodologies incorporates a nanoscale-arranged three- or four-dimensional printing of multicomponent, multifunctional nanostructures, and they are required to pave new roads from the current sensor design [147]. MONPs can be manufactured and evaluated in a variety of configurations, such as sensor arrays, to facilitate the production of functional integrated devices [80]. For this reason, efforts should be made to overcome certain important technological limits such as regulating the morphology of MONPs on devices to commercialize enzymatic biosensors based on MONPs. Additionally, work should be carried out to recognize optimal enzyme immobilization, maintain the enzyme's long-term bioactivity, and reduce matrix interference and sensor fouling [249]. Nanotechnology has changed the nature of biological detection through the advancement of biosensors. The future is bright for this dynamic, flexible, and fast recognition framework, considering the multidimensional capability of nanomaterials and nanostructures. With the momentous progress and thorough research speed of nanomaterial investigation, the detection technology has grown increasingly flexible, robust, and dynamic, and the expanding headway of miniaturization and nanomaterials research has invigorated the utilization of these materials for detecting a few key pathways and regulatory occasions [175]. Ongoing progressions in biosensing platforms have utilized different novel types of nanomaterials, going from monomolecular nanomotors to generally bigger nanocages, so the quick, financially savvy, and easy functional procedures achieved by nanomaterial-based biosensors are required to redesign current detecting frameworks and their pricing.

Funding: This research received no external funding.

Conflicts of Interest: The authors declare no conflicts of interest.

References

1. Schackart, K.E., III; Yoon, J.Y. Machine learning enhances the performance of bioreceptor-free biosensors. *Sensors* **2021**, *21*, 5519. [[CrossRef](#)] [[PubMed](#)]
2. Khan, A.; Rao, T.S. Nanobiosensors for virus detection in the environment. In *Nanomaterials for Air Remediation*; Elsevier: Amsterdam, The Netherlands, 2020; pp. 61–87.

3. Ratajczak, K.; Stobiecka, M. High-performance modified cellulose paper-based biosensors for medical diagnostics and early cancer screening: A concise review. *Carbohydr. Polym.* **2020**, *229*, 115463. [[CrossRef](#)] [[PubMed](#)]
4. Naresh, V.; Lee, N. A review on biosensors and recent development of nanostructured materials-enabled biosensors. *Sensors* **2021**, *21*, 1109. [[CrossRef](#)] [[PubMed](#)]
5. Kaushik, S.; Tiwari, U.K.; Deep, A.; Sinha, R.K. Two-dimensional transition metal dichalcogenides assisted biofunctionalized optical fiber SPR biosensor for efficient and rapid detection of bovine serum albumin. *Sci. Rep.* **2019**, *9*, 6987. [[CrossRef](#)]
6. Sin, M.L.Y.; Mach, K.E.; Wong, P.K.; Liao, J.C. Advances and challenges in the biosensor-based diagnosis of infectious diseases. *Expert Rev. Mol. Diagn.* **2014**, *14*, 225–244. [[CrossRef](#)]
7. Ramesh, M.; Janani, R.; Deepa, C.; Rajeshkumar, L. Nanotechnology-Enabled Biosensors: A Review of Fundamentals, Design Principles, Materials, and Applications. *Biosensors* **2023**, *13*, 40. [[CrossRef](#)]
8. Chai, Z.; Childress, A.; Busnaina, A.A. Directed Assembly of Nanomaterials for Making Nanoscale Devices and Structures: Mechanisms and Applications. *ACS Nano* **2022**, *16*, 17641–17686. [[CrossRef](#)]
9. Dvir, T.; Timko, B.P.; Kohane, D.S.; Langer, R. Nanotechnological strategies for engineering complex tissues. In *Nano-Enabled Medical Applications*; Jenny Stanford Publishing: Singapore, 2020; pp. 351–382.
10. Ejeian, F.; Etedali, P.; Mansouri-Tehrani, H.A.; Soozanipour, A.; Low, Z.X.; Asadnia, M.; Taheri-Kafrani, A.; Razmjou, A. Biosensors for wastewater monitoring: A review. *Biosens. Bioelectron.* **2018**, *118*, 66–79. [[CrossRef](#)]
11. Gözübenli, N. Nano-templated films from waste optical discs for self-powered biosensor application and environmental surveillance. *Appl. Nanosci.* **2020**, *10*, 199–212. [[CrossRef](#)]
12. Wang, Q.; Xue, Q.; Chen, T.; Li, J.; Liu, Y.; Shan, X.; Liu, F.; Jia, J. Recent advances in electrochemical sensors for antibiotics and their applications. *Chin. Chem. Lett.* **2021**, *32*, 609–619. [[CrossRef](#)]
13. Bukkittar, S.D.; Kumar, S.; Singh, S.; Singh, V.; Reddy, K.R.; Sadhu, V.; Bagihalli, G.B.; Shetti, N.P.; Reddy, C.V.; Ravindranadh, K.; et al. Functional nanostructured metal oxides and its hybrid electrodes—Recent advancements in electrochemical biosensing applications. *Microchem. J.* **2020**, *159*, 105522. [[CrossRef](#)]
14. Agnihotri, A.S.; Varghese, A.; Nidhin, M. Transition metal oxides in electrochemical and biosensing: A state-of-art review. *Appl. Surf. Sci. Adv.* **2021**, *4*, 100072. [[CrossRef](#)]
15. Saeb, E.; Asadpour-Zeynali, K. Facile synthesis of TiO₂@PANI@ Au nanocomposite as an electrochemical sensor for determination of hydrazine. *Microchem. J.* **2021**, *160*, 105603. [[CrossRef](#)]
16. Beitollahi, H.; Tajik, S.; Nejad, F.G.; Safaei, M. Recent advances in ZnO nanostructure-based electrochemical sensors and biosensors. *J. Mater. Chem. B* **2020**, *8*, 5826–5844. [[CrossRef](#)]
17. Napi, M.L.M.; Sultan, S.M.; Ismail, R.; How, K.W.; Ahmad, M.K. Electrochemical-based biosensors on different zinc oxide nanostructures: A review. *Materials* **2019**, *12*, 2985. [[CrossRef](#)]
18. Li, X.; Yang, Y.; Zhang, B.; Lin, X.; Fu, X.; An, Y.; Zou, Y.; Wang, J.X.; Wang, Z.; Yu, T. Lactate metabolism in human health and disease. *Signal Transduct. Target. Ther.* **2022**, *7*, 305. [[CrossRef](#)]
19. Yang, W.H.; Park, H.; Grau, M.; Heine, O. Decreased Blood Glucose and Lactate: Is a Useful Indicator of Recovery Ability in Athletes? *Int. J. Environ. Res. Public Health* **2022**, *17*, 5470. [[CrossRef](#)]
20. Khor, S.M.; Choi, J.; Won, P.; Ko, S.H. Challenges and Strategies in Developing an Enzymatic Wearable Sweat Glucose Biosensor as a Practical Point-Of-Care Monitoring Tool for Type II Diabetes. *Nanomaterials* **2022**, *12*, 221. [[CrossRef](#)]
21. Shen, Y.; Liu, C.; He, H.; Zhang, M.; Wang, H.; Ji, K.; Wei, L.; Mao, X.; Sun, R.; Zhou, F. Recent Advances in Wearable Biosensors for Non-Invasive Detection of Human Lactate. *Biosensors* **2022**, *12*, 1164. [[CrossRef](#)]
22. Kim, S.; Yang, W.S.; Kim, H.J.; Lee, H.N.; Park, T.J.; Seo, S.J.; Park, Y.M. Highly sensitive non-enzymatic lactate biosensor driven by porous nanostructured nickel oxide. *Ceram. Int.* **2019**, *45*, 23370–23376. [[CrossRef](#)]
23. Heo, S.G.; Yang, W.S.; Kim, S.; Park, Y.M.; Park, K.T.; Oh, S.J.; Seo, S.J. Synthesis, characterization and non-enzymatic lactate sensing performance investigation of mesoporous copper oxide (CuO) using inverse micelle method. *Appl. Surf. Sci.* **2021**, *555*, 149638. [[CrossRef](#)]
24. Chen, C.C.; Do, J.S.; Gu, Y. Immobilization of HRP in Mesoporous Silica and Its Application for the Construction of Polyaniline Modified Hydrogen Peroxide Biosensor. *Sensors* **2009**, *9*, 4635–4648. [[CrossRef](#)] [[PubMed](#)]
25. Hosu, O.; Tertis, M.; Cristea, C. Implication of magnetic nanoparticles in cancer detection, screening and treatment. *Magnetochemistry* **2019**, *5*, 55. [[CrossRef](#)]
26. Sabrin, S.; Karmakar, D.K.; Karmakar, N.C.; Hong, S.H.; Habibullah, H.; Szili, E.J. Opportunities of Electronic and Optical Sensors in Autonomous Medical Plasma Technologies. *ACS Sens.* **2023**, *8*, 974–993. [[CrossRef](#)] [[PubMed](#)]
27. Khonina, S.N.; Kazanskiy, N.L.; Butt, M.A. Optical Fibre-Based Sensors—An Assessment of Current Innovations. *Biosensors* **2023**, *13*, 835. [[CrossRef](#)]
28. Sharma, P.S.; Choudhury, K.; Gupta, V.K.; Kumar, S. Low-cost fabrication and characterization process for development of a sensitive optical fiber structure. *Appl. Opt. Eng. Lab. Note* **2022**, *61*, 8057.

29. Ahmed, A.; Rushworth, J.V.; Hirst, N.A.; Millner, P.A. Biosensors for Whole-Cell Bacterial Detection. *Clin. Microbiol. Rev.* **2014**, *27*, 631–646. [[CrossRef](#)]
30. Lei, Z.L.; Guo, B. 2D material-based optical biosensor: Status and prospect. *Adv. Sci.* **2022**, *9*, 2102924. [[CrossRef](#)]
31. Akcinar, H.Y.; Aslim, B.; Torul, H.; Güven, B.; Zengin, A.; Suludere, Z.; Boyaci, I.H.; Tamer, U. Immunomagnetic separation and *Listeria monocytogenes* detection with surface-enhanced Raman scattering. *Turk. J. Med. Sci.* **2020**, *50*, 1157–1167. [[CrossRef](#)]
32. Yildirim, N.; Long, F.; Gu, A.Z. Aptamer based E-coli detection in wastewaters by portable optical biosensor system. In Proceedings of the 40th Annual Northeast Bioengineering Conference, IEEE, Boston, MA, USA, 25–27 April 2014; pp. 1–3.
33. Bashi, Z.B.; Büyükkaksoy, A.; Ölmezcan, S.M.; Şimşek, F.; Aslan, M.H.; Oral, A.Y. A Novel Label-Free Optical Biosensor Using Synthetic Oligonucleotides from *E. coli* O157:H7: Elementary Sensitivity Tests. *Sensors* **2009**, *9*, 4890–4900. [[CrossRef](#)]
34. Wu, S.; Duan, N.; Qiu, Y.; Li, J.; Wang, Z. Colorimetric aptasensor for the detection of *Salmonella enterica serovar typhimurium* using ZnFe₂O₄-reduced graphene oxide nanostructures as an effective peroxidase mimetics. *Int. J. Food Microbiol.* **2017**, *261*, 42–48. [[CrossRef](#)] [[PubMed](#)]
35. Ko, Y.C.; Fang, H.Y.; Chen, D.H. Fabrication of Ag/ZnO/reduced graphene oxide nanocomposite for SERS detection and multiway killing of bacteria. *J. Alloys Compd.* **2017**, *695*, 1145–1153. [[CrossRef](#)]
36. Fallah, H.; Asadishad, T.; Parsanasab, G.M.; Harun, S.W.; Mohammed, W.S.; Yasin, M. Optical Fiber Biosensor toward E-coli Bacterial Detection on the Pollutant Water. *Eng. J.* **2021**, *25*, 1–8. [[CrossRef](#)]
37. Franco, D.; De Plano, L.M.; Rizzo, M.G.; Scibilia, S.; Lentini, G.; Fazio, E.; Neri, F.; Guglielmino, S.P.P.; Mezzasalma, M. Bio-hybrid gold nanoparticles as SERS probe for rapid bacteria cell identification. *Spectrochim. Acta Part A Mol. Biomol. Spectrosc.* **2020**, *224*, 117394. [[CrossRef](#)]
38. Kaur, G.; Paliwal, A.; Tomar, M.; Gupta, V. Detection of *Neisseria meningitidis* using surface plasmon resonance based DNA biosensor. *Biosens. Bioelectron.* **2016**, *78*, 106–110. [[CrossRef](#)]
39. Huang, Y.; Yu, B.; Guo, T.; Guan, B.O. Ultrasensitive and in situ DNA detection in various pH environments based on a microfiber with a graphene oxide linking layer. *RSC Adv.* **2017**, *7*, 13177–13183. [[CrossRef](#)]
40. Chiavaioli, F.; Biswas, P.; Trono, C.; Jana, S.; Bandyopadhyay, S.; Basumallick, N.; Giannetti, A.; Tombelli, S.; Bera, S.; Mallick, A.; et al. Sol–gel-based titania–silica thin film overlay for long period fiber grating-based biosensors. *Anal. Chem.* **2015**, *87*, 12024–12031. [[CrossRef](#)]
41. Tsuda, H.; Urabe, K. Characterization of Long-period Grating Refractive Index Sensors and Their Applications. *Sensors* **2009**, *9*, 4559–4571. [[CrossRef](#)]
42. Kikuchi, M.; Ogasawaran, T.; Fujii, S.; Takeda, S. Application of machine learning for improved accuracy of simultaneous temperature and strain measurements of carbon fiber-reinforced plastic laminates using an embedded tilted fiber Bragg grating sensor. *Compos. Part A Appl. Sci. Manuf.* **2022**, *161*, 107108. [[CrossRef](#)]
43. Liu, L.; Zhang, X.; Zhu, Q.; Li, K.; Lu, Y.; Zhou, X.; Guo, T. Ultrasensitive detection of endocrine disruptors via superfine plasmonic spectral combs. *Light Sci. Appl.* **2021**, *10*, 181. [[CrossRef](#)]
44. Li, Z.; Yang, X.; Zhu, H.; Chiavaioli, F. Sensing performance of fiber-optic combs tuned by nanometric films: New insights and limits. *IEEE Sens. J.* **2021**, *21*, 13305–13315. [[CrossRef](#)]
45. Li, Z.; Bao, Q.; Zhu, J.; Runa, X.; Dai, Y. Generation of leaky mode resonance by metallic oxide nanocoating in tilted fiber-optic gratings. *Opt. Express* **2020**, *28*, 9123. [[CrossRef](#)] [[PubMed](#)]
46. Consales, M.; Quero, G.; Spaziani, S.; Principe, M.; Micco, A.; Galdi, V.; Cutolo, A.; Cusano, A. Metasurface-Enhanced Lab-on-Fiber Biosensors. *Laser Photonics Rev.* **2020**, *14*, 2000180. [[CrossRef](#)]
47. Esposito, F.; Sansone, L.; Srivastava, A.; Baldini, F.; Campopiano, S.; Chiavaioli, F.; Giordano, M.; Giannetti, A.; Iadicco, A. Long period grating in double cladding fiber coated with graphene oxide as high-performance optical platform for biosensing. *Biosens. Bioelectron.* **2021**, *172*, 112747. [[CrossRef](#)]
48. Giaquinto, M.; Aliberti, A.; Micco, A.; Gambino, F.; Ruvo, M.; Ricciardi, A.; Cusano, A. Cavity-enhanced lab-on-fiber technology: Toward advanced biosensors and nano-opto-mechanical active devices. *ACS Photonics* **2019**, *6*, 3271–3280. [[CrossRef](#)]
49. Honig, L.S.; Tang, M.X.; Albert, S.; Costa, R.; Luchsinger, J.; Manly, J.; Stern, Y.; Mayeux, R. Stroke and the Risk of Alzheimer Disease. *Arch. Neurol.* **2003**, *60*, 1707–1712. [[CrossRef](#)]
50. Chiavaioli, F.; Santano Rivero, D.; Del Villar, I.; Socorro-Lerános, A.B.; Zhang, X.; Li, K.; Santamaría, E.; Fernández-Irigoyen, J.; Baldini, F.; Van den Hove, D.L.A.; et al. Ultrahigh Sensitive Detection of Tau Protein as Alzheimer’s Biomarker via Microfluidics and Nanofunctionalized Optical Fiber Sensors. *Adv. Photonics Res.* **2022**, *3*, 2200044. [[CrossRef](#)]
51. Chiavaioli, F.; Zubiato, P.; Del Villar, I.; Zamarreño, C.R.; Giannetti, A.; Tombelli, S.; Trono, C.; Arregui, F.J.; Matias, I.R.; Baldini, F. Femtomolar detection by nanocoated fiber label-free biosensors. *ACS Sens.* **2018**, *3*, 936–943. [[CrossRef](#)]
52. Zubiato, P.; Urrutia, A.; Zamarreño, C.R.; Egea-Urra, J.; Fernández-Irigoyen, J.; Giannetti, A.; Baldini, F.; Díaz, S.; Matias, I.R.; Arregui, F.J.; et al. Fiber-based early diagnosis of venous thromboembolic disease by label-free D-dimer detection. *Biosens. Bioelectron. X* **2019**, *2*, 100026. [[CrossRef](#)]

53. Villar, I.D.; Arregui, F.J.; Zamarreño, C.R.; Corres, J.M.; Barriain, C.; Goicoechea, J.; Elosua, C.; Hernaez, M.; Rivero, P.J.; Socorro, A.B.; et al. Optical sensors based on lossy-mode resonances. *Sens. Actuators B* **2017**, *240*, 174–185. [[CrossRef](#)]
54. Moro, G.; Chiavaioli, F.; Liberi, S.; Zubiato, P.; Del Villar, I.; Angelini, A.; De Wael, K.; Baldini, F.; Moretto, L.M.; Giannetti, A. Nanocoated fiber label-free biosensing for perfluorooctanoic acid detection by lossy mode resonance. *Results Opt.* **2021**, *5*, 100123. [[CrossRef](#)]
55. Abdelghaffar, M.; Gamal, Y.; El-Khoribi, R.A.; Soliman, W.; Badr, Y.; Hameed, M.F.O.; Obayya, S.S.A. Cancer cell detection by plasmonic dual V-shaped PCF biosensor. *J. Opt. Soc. Am. B* **2024**, *41*, 222. [[CrossRef](#)]
56. Gunatilake, U.B.; Garcia-Rey, S.; Ojeda, E.; Basabe-Desomonts, L.; Benito-Lopez, F. TiO₂ Nanotubes Alginate Hydrogel Scaffold for Rapid Sensing of Sweat Biomarkers: Lactate and Glucose. *ACS Appl. Mater. Interfaces* **2021**, *13*, 37734–37745. [[CrossRef](#)]
57. Salvo, P.; Vivaldi, F.M.; Bonini, A.; Biagini, D.; Bellagambi, F.G.; Miliani, F.M.; Di Francesco, F.; Lomonaco, T. Biosensors for Detecting Lymphocytes and Immunoglobulins. *Biosensors* **2020**, *10*, 155. [[CrossRef](#)]
58. Saber, R.; Piskin, E. Investigation of complexation of immobilized metallothionein with Zn(II) and Cd(II) ions using piezoelectric crystals. *Biosens. Bioelectron.* **2003**, *18*, 1039–1046. [[CrossRef](#)]
59. Marrazza, G. Piezoelectric biosensors for organophosphate and carbamate pesticides: A review. *Biosensors* **2014**, *4*, 301–317. [[CrossRef](#)]
60. Narita, F.; Wang, Z.; Kurita, H.; Li, Z.; Shi, Y.; Jia, Y.; Soutis, C. A review of piezoelectric and magnetostrictive biosensor materials for detection of COVID-19 and other viruses. *Adv. Mater.* **2021**, *33*, 2005448. [[CrossRef](#)]
61. Pohanka, M. Overview of piezoelectric biosensors, immunosensors and DNA sensors and their applications. *Materials* **2018**, *11*, 448. [[CrossRef](#)]
62. Yuan, M.; Zhang, Q.; Song, Z.; Ye, T.; Yu, J.; Cao, H.; Xu, F. Piezoelectric arsenite aptasensor based on the use of a self-assembled mercaptoethylamine monolayer and gold nanoparticles. *Microchim. Acta* **2019**, *186*, 268. [[CrossRef](#)]
63. Wang, H.; Cai, H.-H.; Zhang, L.; Cai, J.; Yang, P.-H.; Chen, Z.W. A novel gold nanoparticle-doped polyaniline nanofibers-based cytosensor confers simple and efficient evaluation of T-cell activation. *Biosens. Bioelectron.* **2013**, *50*, 167–173. [[CrossRef](#)]
64. Zhao, Y.; Fu, Y.; Wang, P.; Xing, L.; Xue, X. Highly stable piezo-immunoglobulin-biosensing of a SiO₂/ZnO nanogenerator as a self-powered/active biosensor arising from the field effect influenced piezoelectric screening effect. *Nanoscale* **2015**, *7*, 1904–1911. [[CrossRef](#)] [[PubMed](#)]
65. Vasuki, S.; Varsha, V.; Mithra, R.; Dharshni, R.A.; Abinaya, S.; Dharshini, R.D.; Sivarajasekar, N. Thermal biosensors and their applications. *Am. Int. J. Res. Sci. Tech. Eng. Math.* **2019**, *1*, 262–264.
66. Arya, A.; Gangwar, A.; Kumar, A. Biosensors in animal biotechnology. In *Nanotechnology in Modern Animal Biotechnology: Concepts and Applications*, 1st ed.; Maurya, P.K., Singh, S., Eds.; Elsevier: Cambridge, MA, USA, 2019; pp. 75–95.
67. Soni, T.; Vivekanand, V.; Pareek, N. Biosensors as an effective tool for detection of emerging water and wastewater pollutants. In *Biodegradation and Detoxification of Micropollutants in Industrial Wastewater*; Elsevier: Amsterdam, The Netherlands, 2022; pp. 39–54.
68. Mughal, S.S.; Hassan, S.M. Comparative Study of AgO Nanoparticles Synthesize Via Biological, Chemical and Physical Methods: A Review. *Am. J. Mater. Synth. Process.* **2022**, *7*, 15–28.
69. Xu, Y.; Zheng, L.; Yang, C.; Zheng, W.; Liu, X.; Zhang, J. Chemiresistive sensors based on core-shell ZnO@TiO₂ nanorods designed by atomic layer deposition for n-butanol detection. *Sens. Actuators B Chem.* **2020**, *310*, 127846. [[CrossRef](#)]
70. Ali, I.; Kashyout, A.E.H.B.; Tayel, M.; Hassan, H.S.; Rizk, M. Ruthenium (Ru) doped zinc oxide nanostructure-based radio frequency identification (RFID) gas sensors for NH₃ detection. *J. Mater. Res. Technol.* **2020**, *9*, 15693–15704. [[CrossRef](#)]
71. Ghasemi-Varnamkhashti, M.; Amiri, Z.S.; Tohidi, M.; Dowlati, M.; Mohtasebi, S.S.; Silva, A.C.; Fernandes, D.D.S.; Araujo, M.C. Differentiation of cumin seeds using a metal-oxide-based gas sensor array in tandem with chemometric tools. *Talanta* **2018**, *176*, 221–226. [[CrossRef](#)]
72. Khaliq, N.; Rasheed, M.A.; Cha, G.; Khan, M.; Karim, S.; Schmuki, P.; Ali, G. Development of non-enzymatic cholesterol bio-sensor based on TiO₂ nanotubes decorated with Cu₂O nanoparticles. *Sens. Actuators B Chem.* **2020**, *302*, 127200. [[CrossRef](#)]
73. Fazio, E.; Spadaro, S.; Corsaro, C.; Neri, G.; Leonardi, S.G.; Neri, F.; Lavanya, N.; Sekar, C.; Donato, N.; Neri, G. Metal-Oxide Based Nanomaterials: Synthesis, Characterization and Their Applications in Electrical and Electrochemical Sensors. *Sensors* **2021**, *21*, 2494. [[CrossRef](#)]
74. Chavali, M.S.; Nikolova, M.P. Metal oxide nanoparticles and their applications in nanotechnology. *SN Appl. Sci.* **2019**, *1*, 607. [[CrossRef](#)]
75. Solanki, P.R.; Kaushik, A.; Agrawal, V.V.; Malhotra, B.D. Nanostructured metal oxide-based biosensors. *NPG Asia Mater.* **2011**, *3*, 17–24. [[CrossRef](#)]
76. . Rim, Y.S. Review of metal oxide semiconductors-based thin-film transistors for point-of-care sensor applications. *J. Inf. Disp.* **2020**, *21*, 203–210. [[CrossRef](#)]
77. Farsi, M.; Nezamzadeh-Ejhieh, A. A coupled Cobalt (II) oxide-Silver Tungstate nano-photocatalyst: Moderate characterization and evaluation of the photocatalysis kinetics towards methylene blue in aqueous solution. *Polyhedron* **2022**, *219*, 115823. [[CrossRef](#)]

78. George, J.M.; Antony, A.; Mathew, B. Metal oxide nanoparticles in electrochemical sensing and biosensing: A review. *Microchim. Acta* **2018**, *185*, 1–26. [[CrossRef](#)]
79. Johnson, A.P.; Sabu, C.; Nivitha, K.P.; Sankar, R.; Shirin, V.A.; Henna, T.K.; Raphey, V.R.; Gangadharappa, H.V.; Kotta, S.; Pramod, K. Bioinspired and biomimetic micro- and nanostructures in biomedicine. *J. Control. Release* **2022**, *343*, 724–754. [[CrossRef](#)]
80. Ren, X.; Meng, X.; Chen, D.; Tang, F.; Jiao, J. Using silver nanoparticle to enhance current response of biosensor. *Biosens. Bioelectron.* **2005**, *21*, 433–437. [[CrossRef](#)]
81. Charbgoon, F.; Ahmad, M.B.; Darroudi, M. Cerium oxide nanoparticles: Green synthesis and biological applications. *Int. J. Nanomed.* **2017**, *12*, 1401–1413. [[CrossRef](#)]
82. Verma, N.; Kumar, N. Synthesis and biomedical applications of copper oxide nanoparticles: An expanding horizon. *ACS Biomater. Sci. Eng.* **2019**, *5*, 1170–1188. [[CrossRef](#)]
83. Theerthagiri, J.; Salla, S.; Senthil, R.A.; Nithyadharseni, P.; Madankumar, A.; Arunachalam, P.; Maiyalagan, T.; Kim, H.S. A review on ZnO nanostructured materials: Energy, environmental and biological applications. *Nanotechnology* **2019**, *30*, 392001. [[CrossRef](#)]
84. Manna, A.K.; Guha, P.; Solanki, V.J.; Srivastava, S.K.; Varma, S. Non-enzymatic glucose sensing with hybrid nanostructured Cu₂O-ZnO prepared by single-step electrodeposition technique. *J. Solid State Electrochem.* **2020**, *24*, 1647–1658. [[CrossRef](#)]
85. Ahmad, R.; Tripathy, N.; Ahn, M.S.; Bhat, K.S.; Mahmoudi, T.; Wang, Y.; Yoo, J.Y.; Kwon, D.W.; Yang, H.Y.; Hahn, Y.B. Highly efficient non-enzymatic glucose sensor based on CuO-modified vertically-grown ZnO nanorods on electrode. *Sci. Rep.* **2017**, *7*, 5715. [[CrossRef](#)]
86. Devi, R.; Yadav, S.; Pundir, C.S. Amperometric determination of xanthine in fish meat by zinc oxide nanoparticle/chitosan/multiwalled carbon nanotube/polyaniline composite film bound xanthine oxidase. *Analyst* **2012**, *137*, 754–759. [[CrossRef](#)] [[PubMed](#)]
87. Al-Douri, Y.; Gherab, K.; Batoo, K.M.; Raslan, E.H. Detecting the DNA of dengue serotype 2 using aluminum nanoparticle doped zinc oxide nanostructure: Synthesis, analysis and characterization. *J. Mater. Res. Technol.* **2020**, *9*, 5515–5523. [[CrossRef](#)]
88. Nien, Y.H.; Kang, Z.X.; Su, T.Y.; Ho, C.S.; Chou, J.C.; Lai, C.H.; Dong, Z.X.; Chen, Y.Y.; Huang, Y.H. Investigation of flexible arrayed lactate biosensor based on copper-doped zinc oxide films modified by iron-platinum nanoparticles. *Polymers* **2021**, *13*, 2062. [[CrossRef](#)] [[PubMed](#)]
89. Gupta, V.K.; Norouzi, P.; Ganjali, H.; Faridbod, F.; Ganjali, M.R. Flow injection analysis of cholesterol using FFT admittance voltammetric biosensor based on MWCNT-ZnO nanoparticles. *Electrochim. Acta* **2013**, *100*, 29–34. [[CrossRef](#)]
90. Ghanei Agh Kaariz, D.; Darabi, E.; Elahi, S.M. Fabrication of Au/ZnO/MWCNTs electrode and its characterization for electrochemical cholesterol biosensor. *J. Theor. Appl. Phys.* **2020**, *14*, 339–348. [[CrossRef](#)]
91. Rajeshkumar, S.; Lakshmi, T.; Naik, P. Recent advances and biomedical applications of zinc oxide nanoparticles. In *Green Synthesis, Characterization and Applications of Nanoparticles*; Elsevier: Amsterdam, The Netherlands, 2019; pp. 445–457.
92. Vasudevan, S.; Srinivasan, P.; Rayappan, J.B.B.; Solomon, A.P. A photoluminescence biosensor for the detection of N-acyl homoserine lactone using cysteamine functionalized ZnO nanoparticles for the early diagnosis of urinary tract infections. *J. Mater. Chem. B* **2020**, *8*, 4228–4236. [[CrossRef](#)]
93. Nagal, V.; Kumar, V.; Khan, M.; Alomar, S.Y.; Tripathy, N.; Singh, K.; Khosla, A.; Ahmad, N.; Hafiz, A.K.; Ahmad, R. A highly sensitive uric acid biosensor based on vertically arranged ZnO nanorods on a ZnO nanoparticle-seeded electrode. *New J. Chem.* **2021**, *45*, 18863–18870. [[CrossRef](#)]
94. Zheng, R.; Zhao, C.; Zhong, J.; Qiu, Z.; Hu, Z. Determination of epinephrine using a novel sensitive electrochemiluminescence sensor based on ZnO nanoparticles modified pencil graphite electrode. *Int. J. Electrochem. Sci.* **2019**, *14*, 9380–9390. [[CrossRef](#)]
95. Migliorini, F.L.; Sanfelice, R.C.; Mercante, L.A.; Andre, R.S.; Mattoso, L.H.; Correa, D.S. Urea impedimetric biosensing using electrospun nanofibers modified with zinc oxide nanoparticles. *Appl. Surf. Sci.* **2018**, *443*, 18–23. [[CrossRef](#)]
96. Tesfaye, G.; Negash, N.; Tessema, M. Sensitive and selective determination of vitamin B2 in non-alcoholic beverage and milk samples at poly (glutamic acid)/zinc oxide nanoparticles modified carbon paste electrode. *BMC Chem.* **2022**, *16*, 1–17. [[CrossRef](#)]
97. Ghosh, J.; Ghosh, R.; Giri, P.K. Tuning the visible photoluminescence in Al-doped ZnO thin film and its application in label-free glucose detection. *Sens. Actuators B Chem.* **2018**, *254*, 681–689. [[CrossRef](#)]
98. Shukla, S.K.; Deshpande, S.R.; Shukla, S.K.; Tiwari, A. Fabrication of a tunable glucose biosensor based on zinc oxide/chitosan-graft-poly (vinyl alcohol) core-shell nanocomposite. *Talanta* **2012**, *99*, 283–287. [[CrossRef](#)] [[PubMed](#)]
99. Dakshayini, B.S.; Reddy, K.R.; Mishra, A.; Shetti, N.P.; Malode, S.J.; Basu, S.; Naveen, S.; Raghu, A.V. Role of conducting polymer and metal oxide-based hybrids for applications in amperometric sensors and biosensors. *Microchem. J.* **2019**, *147*, 7–24. [[CrossRef](#)]
100. Hussain, M.M.; Asiri, A.M.; Rahman, M.M. Non-enzymatic simultaneous detection of acetylcholine and ascorbic acid using ZnO-CuO nanoleaves: Real sample analysis. *Microchem. J.* **2020**, *159*, 105534. [[CrossRef](#)]
101. Lane, R.M.; Kivipelto, M.; Greig, N.H. Acetylcholinesterase and its inhibition in Alzheimer's disease. *Clin. Neuropharmacol.* **2004**, *27*, 141–149. [[CrossRef](#)]
102. Hanani, M.; Spray, D.C. Emerging importance of satellite glia in nervous system function and dysfunction. *Nat. Rev. Neurosci.* **2020**, *21*, 485–498. [[CrossRef](#)]

103. Zheng, H.; Youdim, M.B.; Fridkin, M. Site-activated multifunctional chelator with acetylcholinesterase and neuroprotective–neurorestorative moieties for Alzheimer’s therapy. *J. Med. Chem.* **2009**, *52*, 4095–4098. [[CrossRef](#)]
104. Vinotha, V.; Yazhiniprabha, M.; Jeyavani, J.; Vaseeharan, B. Synthesis and characterization of cry protein coated zinc oxide nanocomposites and its assessment against bacterial biofilm and mosquito vectors. *Int. J. Biol. Macromol.* **2022**, *208*, 935–947. [[CrossRef](#)]
105. Kaya, S.I.; Kurbanoglu, S.; Ozkan, S.A. Nanomaterials-based nanosensors for the simultaneous electrochemical determination of biologically important compounds: Ascorbic acid, uric acid, and dopamine. *Crit. Rev. Anal. Chem.* **2019**, *49*, 101–125. [[CrossRef](#)]
106. Reddy, S.L.; Arul, C.; Zhaoqi, L.; Lavanya, N.; Sekar, C. A novel electrochemical sensor based on Fe-doped MgNi₂O₃ nanoparticles for simultaneous determination of dopamine, uric acid, nicotine and caffeine over very wide linear ranges. *J. Electroanal. Chem.* **2020**, *878*, 114648. [[CrossRef](#)]
107. Avinash, B.; Ravikumar, C.R.; Kumar, M.A.; Nagaswarupa, H.P.; Santosh, M.S.; Bhatt, A.S.; Kuznetsov, D. Nano CuO: Electrochemical sensor for the determination of paracetamol and D-glucose. *J. Phys. Chem. Solids* **2019**, *134*, 193–200. [[CrossRef](#)]
108. Shanmugam, P.; Kuppuswamy, G.P.; Pushparaj, K.; Arumugam, B.; Sundaramurthy, A.; Sivalingam, Y. CeO₂ nanoparticles based extended gate field effect transistor for enzyme free detection of glucose. *J. Mater. Sci. Mater. Electron.* **2022**, *33*, 9483–9489. [[CrossRef](#)]
109. Fallatah, A.; Almomtan, M.; Padalkar, S. Cerium oxide-based glucose biosensors: Influence of morphology and underlying substrate on biosensor performance. *ACS Sustain. Chem. Eng.* **2019**, *7*, 8083–8089. [[CrossRef](#)]
110. Zhou, Y.; Uzun, S.D.; Watkins, N.J.; Li, S.; Li, W.; Briseno, A.L.; Watkins, J.J. Three-dimensional CeO₂ woodpile nanostructures to enhance performance of enzymatic glucose biosensors. *ACS Appl. Mater. Interfaces* **2018**, *11*, 1821–1828. [[CrossRef](#)]
111. Wang, H.; Yang, W.; Wang, X.; Huang, L.; Zhang, Y.; Yao, S. A CeO₂@ MnO₂ core-shell hollow heterojunction as glucose oxidase-like photoenzyme for photoelectrochemical sensing of glucose. *Sens. Actuators B Chem.* **2020**, *304*, 127389. [[CrossRef](#)]
112. Nguyet, N.T.; Doan, V.Y.; Hoang, N.L.; Van Thu, V.; Trung, T.; Pham, V.H.; Tam, P.D. A label-free and highly sensitive DNA biosensor based on the core-shell structured CeO₂-NR@ Ppy nanocomposite for Salmonella detection. *Mater. Sci. Eng. C* **2019**, *96*, 790–797. [[CrossRef](#)]
113. Wu, B.; Xiao, L.; Zhang, M.; Yang, C.; Li, Q.; Li, G.; He, Q.; Liu, J. Facile synthesis of dendritic-like CeO₂/rGO composite and application for detection of uric acid and tryptophan simultaneously. *J. Solid State Chem.* **2021**, *296*, 122023. [[CrossRef](#)]
114. Zuo, F.; Zhang, C.; Zhang, H.; Tan, X.; Chen, S.; Yuan, R. A solid-state electrochemiluminescence biosensor for Con A detection based on CeO₂@ Ag nanoparticles modified graphene quantum dots as signal probe. *Electrochim. Acta* **2019**, *294*, 76–83. [[CrossRef](#)]
115. Alim, S.; Kafi, A.K.M.; Rajan, J.; Yusoff, M.M. Application of polymerized multiporous nanofiber of SnO₂ for designing a bienzyme glucose biosensor based on HRP/GOx. *Int. J. Biol. Macromol.* **2019**, *123*, 1028–1034. [[CrossRef](#)]
116. Lin, Z.; Wu, G.; Zhao, L.; Lai, K.W.C. Carbon nanomaterial-based biosensors: A review of design and applications. *IEEE Nanotechnol. Mag.* **2019**, *13*, 4–14. [[CrossRef](#)]
117. Wang, Y.; Sun, Y.; Dai, H.; Ni, P.; Jiang, S.; Lu, W.; Li, Z. A colorimetric biosensor using Fe₃O₄ nanoparticles for highly sensitive and selective detection of tetracyclines. *Sens. Actuators B Chem.* **2016**, *236*, 621–626. [[CrossRef](#)]
118. Manbohi, A.; Ahmadi, S.H. Chitosan–Fe₃O₄ nanoparticle enzymatic electrodes on paper as an efficient assay for glucose and uric acid detection in biological fluids. *Chem. Pap.* **2020**, *74*, 2675–2687. [[CrossRef](#)]
119. Hazra, R.S.; Kale, N.; Aland, G.; Qayyumi, B.; Mitra, D.; Jiang, L.; Bajwa, D.; Khandare, J.; Chaturvedi, P.; Quadir, M. Cellulose Mediated transferrin nanocages for enumeration of circulating tumor cells for Head and neck cancer. *Sci. Rep.* **2020**, *10*, 10010.
120. Sun, Y.; Xu, L.; Liu, X.; Shen, Y.; Zhang, Y.; Gu, N.; Xiong, F. Coronal relay reactor Fe₃O₄@ CeO₂ for accelerating ROS axial conversion through enhanced Enzyme-like effect and relay effect. *Chem. Eng. J.* **2022**, *429*, 132303. [[CrossRef](#)]
121. Pezhhan, H.; Akhond, M.; Shamsipur, M. A novel nanoplatfrom encapsulating glucose oxidase for spectrophotometric biosensing of hydrogen peroxide and glucose. *Anal. Methods* **2020**, *12*, 345–357. [[CrossRef](#)]
122. Lang, R.A. Analysis and Optimization of Calorimetric Nanosensors for Rapid Detection of Microbes in Water. Master’s Thesis, California Polytechnic State University, San Luis Obispo, CA, USA, 2020.
123. Apak, R.; Çapanoğlu, E.; Arda, A.Ü. Nanotechnological Methods of Antioxidant Characterization. In *The Chemical Sensory Informatics of Food: Measurement, Analysis, Integration*; American Chemical Society: Washington, DC, USA, 2015; pp. 209–234.
124. Jang, H.D.; Kim, S.K.; Chang, H.; Roh, K.M.; Choi, J.W.; Huang, J. A glucose biosensor based on TiO₂–graphene composite. *Biosens. Bioelectron.* **2012**, *38*, 184–188. [[CrossRef](#)]
125. Cui, H.F.; Zhang, T.T.; Lv, Q.Y.; Song, X.; Zhai, X.J.; Wang, G.G. An acetylcholinesterase biosensor based on doping Au nanorod@ SiO₂ nanoparticles into TiO₂-chitosan hydrogel for detection of organophosphate pesticides. *Biosens. Bioelectron.* **2019**, *141*, 111452. [[CrossRef](#)]
126. Sakib, S.; Pandey, R.; Soleymani, L.; Zhitomirsky, I. Surface modification of TiO₂ for photoelectrochemical DNA biosensors. *Med. Devices Sens.* **2020**, *3*, e10066. [[CrossRef](#)]

127. Wang, Q.; Gao, F.; Zhang, X.; Zhang, B.; Li, S.; Hu, Z.; Gao, F. Electrochemical characterization and DNA sensing application of a sphere-like CeO₂-ZrO₂ and chitosan nanocomposite formed on a gold electrode by one-step electrodeposition. *Electrochim. Acta* **2012**, *62*, 250–255. [[CrossRef](#)]
128. Temerk, Y.; Ibrahim, H. A new sensor based on in doped CeO₂ nanoparticles modified glassy carbon paste electrode for sensitive determination of uric acid in biological fluids. *Sens. Actuators B Chem.* **2016**, *224*, 868–877. [[CrossRef](#)]
129. Wang, G.; Tan, X.; Zhou, Q.; Liu, Y.; Wang, M.; Yang, L. Synthesis of highly dispersed zinc oxide nanoparticles on carboxylic graphene for development a sensitive acetylcholinesterase biosensor. *Sens. Actuators B Chem.* **2014**, *190*, 730–736. [[CrossRef](#)]
130. Hwa, K.Y.; Subramani, B. Synthesis of zinc oxide nanoparticles on graphene-carbon nanotube hybrid for glucose biosensor applications. *Biosens. Bioelectron.* **2014**, *62*, 127–133. [[CrossRef](#)] [[PubMed](#)]
131. Li, M.; Guo, W.; Li, H.; Dai, W.; Yang, B. Electrochemical biosensor based on one-dimensional MgO nanostructures for the simultaneous determination of ascorbic acid, dopamine, and uric acid. *Sens. Actuators B Chem.* **2014**, *204*, 629–636. [[CrossRef](#)]
132. Zhao, L.; Li, H.; Gao, S.; Li, M.; Xu, S.; Li, C.; Yang, B. MgO nanobelt-modified graphene-tantalum wire electrode for the simultaneous determination of ascorbic acid, dopamine and uric acid. *Electrochim. Acta* **2015**, *168*, 191–198. [[CrossRef](#)]
133. Farajpour, N.; Deivanayagam, R.; Phakatkar, A.; Narayanan, S.; Shahbazian-Yassar, R.; Shokuhfar, T. A novel antimicrobial electrochemical glucose biosensor based on silver-Prussian blue-modified TiO₂ nanotube arrays. *Med. Devices Sens.* **2020**, *3*, 10061. [[CrossRef](#)]
134. Yang, W.; Xu, W.; Wang, Y.; Chen, D.; Wang, X.; Cao, Y.; Zhen, C. Photoelectrochemical glucose biosensor based on the heterogeneous facets of nanocrystalline TiO₂/Au/glucose oxidase films. *ACS Appl. Nano Mater.* **2020**, *3*, 2723–2732. [[CrossRef](#)]
135. Ognjanović, M.; Stanković, V.; Knežević, S.; Antić, B.; Vranješ-Djurić, S.; Stanković, D.M. TiO₂/APTES cross-linked to carboxylic graphene based impedimetric glucose biosensor. *Microchem. J.* **2020**, *158*, 105150. [[CrossRef](#)]
136. Yoo, J.; Jeong, H.; Park, S.K.; Park, S.; Lee, J.S. Interdigitated Electrode Biosensor Based on Plasma-Deposited TiO₂ Nanoparticles for Detecting DNA. *Biosensors* **2021**, *11*, 212–222. [[CrossRef](#)]
137. Victorious, A.; Clifford, A.; Saha, S.; Zhitomirsky, I.; Soleymani, L. Integrating TiO₂ nanoparticles within a catecholic polymeric network enhances the photoelectrochemical response of biosensors. *J. Phys. Chem. C* **2019**, *123*, 16186–16193. [[CrossRef](#)]
138. Viticoli, M.; Curulli, A.; Cusma, A.; Kaciulis, S.; Nunziante, S.; Pandolfi, L.; Padeletti, G. Third-generation biosensors based on TiO₂ nanostructured films. *Mater. Sci. Eng. C* **2006**, *26*, 947–951. [[CrossRef](#)]
139. Ghasemi, S.; Bari, M.R.; Pirsá, S.; Amiri, S. Use of bacterial cellulose film modified by polypyrrole/TiO₂-Ag nanocomposite for detecting and measuring the growth of pathogenic bacteria. *Carbohydr. Polym.* **2020**, *232*, 115801. [[CrossRef](#)] [[PubMed](#)]
140. Singh, R.P.; Singh, P.; Singh, K.R. Introduction to Composite Materials: Nanocomposites and Their Potential Applications. In *Composite Materials*; CRC Press: Boca Raton, FL, USA, 2021; pp. 1–28.
141. Kim, W.T.; Choi, W.Y. Optical interference of TiO₂ nanotube arrays for drug elution sensing. *Sci. Adv. Mater.* **2018**, *10*, 283–287. [[CrossRef](#)]
142. Wang, S.; Tang, S.; Gao, H.; Chen, X.; Liu, H.; Yu, C.; Yin, Z.; Zhao, X.; Pan, X.; Yang, H. Microstructure, optical, photoluminescence properties and the intrinsic mechanism of photoluminescence and photocatalysis for the BaTiO₃, BaTiO₃/TiO₂ and BaTiO₃/TiO₂/CeO₂ smart composites. *Opt. Mater.* **2021**, *118*, 111273. [[CrossRef](#)]
143. Mphuthi, N.; Sikhwivhilu, L.; Ray, S.S. Functionalization of 2D MoS₂ Nanosheets with Various Metal and Metal Oxide Nanostructures: Their Properties and Application in Electrochemical Sensors. *Biosensors* **2022**, *12*, 386. [[CrossRef](#)]
144. Shnoudeh, A.J.; Hamad, I.; Abdo, R.W.; Qadumii, L.; Jaber, A.Y.; Surchi, H.S.; Alkelany, S.Z. Synthesis, characterization, and applications of metal nanoparticles. In *Biomaterials and Bionanotechnology*; Academic Press: Cambridge, MA, USA, 2019; pp. 527–612.
145. Șerban, I.; Enesca, A. Metal oxides-based semiconductors for biosensors applications. *Front. Chem.* **2020**, *8*, 354. [[CrossRef](#)]
146. Tripathy, N.; Kim, D.H. Metal oxide modified ZnO nanomaterials for biosensor applications. *Nano Converg.* **2018**, *5*, 27. [[CrossRef](#)]
147. Arya, S.K.; Wong, C.C.; Jeon, Y.J.; Bansal, T.; Park, M.K. Advances in complementary-metal-oxide-semiconductor-based integrated biosensor arrays. *Chem. Rev.* **2015**, *115*, 5116–5158. [[CrossRef](#)]
148. Tran, D.P.; Pham, T.T.T.; Wolfrum, B.; Offenhäusser, A.; Thierry, B. CMOS-compatible silicon nanowire field-effect transistor biosensor: Technology development toward commercialization. *Materials* **2018**, *11*, 785. [[CrossRef](#)]
149. Kutovyi, Y.; Li, J.; Zadorozhnyi, I.; Hlukhova, H.; Boichuk, N.; Yehorov, D.; Menger, M.; Vitusevich, S. Highly sensitive and fast detection of C-reactive protein and troponin biomarkers using liquid-gated single silicon nanowire biosensors. *MRS Adv.* **2020**, *5*, 835–846. [[CrossRef](#)]
150. Kuo, P.Y.; Lai, W.H.; Chen, Y.Y.; Chang, C.H. A Temperature Compensation Circuit Applied to Extended Gate Field Effect Transistor Based on the RuO₂ Ascorbic Acid Sensing Window. *IEEE Trans. Instrum. Meas.* **2022**, *71*, 4002910. [[CrossRef](#)]
151. Tyagi, V.; Bhattacharya, B. Biosensors: Potential in Food Industry. In *Sustainable Agriculture Reviews*; Springer: Berlin/Heidelberg, Germany, 2021; Volume 55, pp. 239–262.
152. Arlett, J.L.; Myers, E.B.; Roukes, M.L. Comparative advantages of mechanical biosensors. *Nat. Nanotechnol.* **2011**, *6*, 203–215. [[CrossRef](#)] [[PubMed](#)]

153. Bertel, L.; Miranda, D.A.; García-Martín, J.M. Nanostructured titanium dioxide surfaces for electrochemical biosensing. *Sensors* **2021**, *21*, 6167. [[CrossRef](#)] [[PubMed](#)]
154. Chhillar, A.K.; Rana, J.S. Enzyme nanoparticles and their biosensing applications: A review. *Anal. Biochem.* **2019**, *581*, 113345.
155. Yue, H.Y.; Zhang, H.J.; Huang, S.; Lu, X.X.; Gao, X.; Song, S.S.; Wang, Z.; Wang, W.Q.; Guan, E.H. Highly sensitive and selective dopamine biosensor using Au nanoparticles-ZnO nanocone arrays/graphene foam electrode. *Mater. Sci. Eng. C* **2020**, *108*, 110490. [[CrossRef](#)]
156. Ali, M.; Shah, I.; Kim, S.W.; Sajid, M.; Lim, J.H.; Choi, K.H. Quantitative detection of uric acid through ZnO quantum dots based highly sensitive electrochemical biosensor. *Sens. Actuators A Phys.* **2018**, *283*, 282–290. [[CrossRef](#)]
157. Dalkıran, B.; Kaçar, C.; Erden, P.E.; Kılıç, E. Electrochemical xanthine biosensor based on zinc oxide nanoparticles-multiwalled carbon nanotubes-1, 4-benzoquinone composite. *J. Turk. Chem. Soc. Sect. A Chem.* **2018**, *5*, 317–332. [[CrossRef](#)]
158. Antonio Tricoli, A.; Neri, G. Miniaturized Bio-and Chemical-Sensors for Point-of-Care Monitoring of Chronic Kidney Diseases. *Sensors* **2018**, *18*, 942. [[CrossRef](#)]
159. Eckfeldt, J.; Levine, A.S.; Greiner, C.; Kershaw, M. Urinary urea: Are currently available methods adequate for revival of an almost abandoned test? *Clin. Chem.* **1982**, *28*, 1500–1502. [[CrossRef](#)]
160. Arain, M.; Nafady, A.; Sirajuddin, C.; Ibupoto, Z.H.; Tufail, S.; Sherazi, H.; Shaikh, T.; Khan, H.; Alsalmeh, A.; Niaz, A.; et al. Simpler and highly sensitive enzyme-free sensing of urea via NiO nanostructures modified electrode. *RSC Adv.* **2016**, *6*, 39001–39006. [[CrossRef](#)]
161. Yoon, J.; Lee, E.; Lee, D.; Oh, T.-S.; Woo, S.P.; Yoon, Y.S.; Kim, D.-J. Non-enzymatic urea detection via using Ag/ZnO nanorod-based catalyst. In *Meeting Abstracts*; The Electrochemical Society: Pennington, NJ, USA, 2017.
162. Devi, S.; Tharmaraj, V. Biosensor Devices Based on Metal Oxide Materials. In *Metal, Metal-Oxides and Metal Sulfides for Batteries, Fuel Cells, Solar Cells, Photocatalysis and Health Sensors. Environmental Chemistry for a Sustainable World*; Rajendran, S., Karimi-Maleh, H., Qin, J., Lichtfouse, E., Eds.; Springer: Cham, Switzerland, 2021.
163. Maruthupandy, M.; Zuo, Y.; Chen, J.S.; Song, J.M.; Niu, H.L.; Mao, C.J.; Shen, Y.H. Synthesis of metal oxide nanoparticles (CuO and ZnO NPs) via biological template and their optical sensor applications. *Appl. Surf. Sci.* **2017**, *397*, 167–174. [[CrossRef](#)]
164. Wahab, H.A.; Salama, A.A.; El Saeid, A.A.; Willander, M.; Nur, O.; Battisha, I.K. Zinc oxide nano-rods based glucose biosensor devices fabrication. *Results Phys.* **2018**, *9*, 809–814. [[CrossRef](#)]
165. Khan, N.; Athar, T.; Fouad, H.; Umar, A.; Ansari, Z.A.; Ansari, S.G. Application of pristine and doped SnO₂ nanoparticles as a matrix for agro-hazardous material (organophosphate) detection. *Sci. Rep.* **2017**, *7*, 42510. [[CrossRef](#)]
166. Parnianchi, F.; Nazari, M.; Maleki, J.; Mohebi, M. Combination of graphene and graphene oxide with metal and metal oxide nanoparticles in fabrication of electrochemical enzymatic biosensors. *Int. Nano Lett.* **2018**, *8*, 229–239. [[CrossRef](#)]
167. Liu, B.; Liu, J. Sensors and biosensors based on metal oxide nanomaterials. *TrAC Trends Anal. Chem.* **2019**, *121*, 115690. [[CrossRef](#)]
168. Kao, C.H.; Chang, C.L.; Su, W.M.; Chen, Y.T.; Lu, C.C.; Lee, Y.S.; Hong, C.H.; Lin, C.Y.; Chen, H. Magnesium oxide (MgO) pH-sensitive sensing membrane in electrolyte-insulator-semiconductor structures with CF₄ plasma treatment. *Sci. Rep.* **2017**, *7*, 7185. [[CrossRef](#)]
169. Vyas, S. A short review on properties and applications of ZnO based thin film and devices. *Johns. Matthey Technol. Rev.* **2020**, *64*, 202–218. [[CrossRef](#)]
170. Khazaei, S.; Mozaffari, S.A.; Ebrahimi, F. Polyvinyl alcohol as a crucial omissible polymer to fabricate an impedimetric glucose biosensor based on hierarchical 3D-NPZnO/chitosan. *Carbohydr. Polym.* **2021**, *266*, 118105. [[CrossRef](#)]
171. Danielson, E.; Dhamodharan, V.; Porkovich, A.; Kumar, P.; Jian, N.; Ziadi, Z.; Sowwan, M. Gas-phase synthesis for label-free biosensors: Zinc-oxide nanowires functionalized with gold nanoparticles. *Sci. Rep.* **2019**, *9*, 17370. [[CrossRef](#)]
172. Supraja, P.; Singh, V.; Vanjari, S.R.K.; Singh, S.G. Electrospun CNT embedded ZnO nanofiber-based biosensor for electrochemical detection of Atrazine: A step closure to single molecule detection. *Microsyst. Nanoeng.* **2020**, *6*, 3. [[CrossRef](#)]
173. Rong, P.; Ren, S.; Yu, Q. Fabrications and applications of ZnO nanomaterials in flexible functional devices—a review. *Crit. Rev. Anal. Chem.* **2019**, *49*, 336–349. [[CrossRef](#)]
174. Xu, Z.; Yuan, Y.J. Implementation of guiding layers of surface acoustic wave devices: A review. *Biosens. Bioelectron.* **2018**, *99*, 500–512. [[CrossRef](#)] [[PubMed](#)]
175. Purohit, B.; Vernekar, P.R.; Shetti, N.P.; Chandra, P. Biosensor nanoengineering: Design, operation, and implementation for biomolecular analysis. *Sens. Int.* **2020**, *1*, 100040. [[CrossRef](#)]
176. Kadadou, D.; Tizani, L.; Wadi, V.S.; Banat, F.; Alsafar, H.; Yousef, A.F.; Barceló, D.; Hasan, S.W. Recent advances in the biosensors application for the detection of bacteria and viruses in wastewater. *J. Environ. Chem. Eng.* **2021**, *10*, 107070. [[CrossRef](#)]
177. Huang, X.; Liu, Y.; Yung, B.; Xiong, Y.; Chen, X. Nanotechnology-enhanced no-wash biosensors for in vitro diagnostics of cancer. *ACS Nano* **2017**, *11*, 5238–5292. [[CrossRef](#)] [[PubMed](#)]
178. Srivastava, M.; Srivastava, N.; Mishra, P.K.; Malhotra, B.D. Prospects of nanomaterials-enabled biosensors for COVID-19 detection. *Sci. Total Environ.* **2021**, *754*, 142363. [[CrossRef](#)]

179. Chen, Z.; Zhang, Z.; Zhai, X.; Li, Y.; Lin, L.; Zhao, H.; Bian, L.; Li, P.; Yu, L.; Wu, Y.; et al. Rapid and Sensitive Detection of anti-SARS-CoV-2 IgG, Using Lanthanide-Doped Nanoparticles-Based Lateral Flow Immunoassay. *Anal. Chem.* **2020**, *92*, 7226–7231. [[CrossRef](#)]
180. Vadlamani, B.S.; Uppal, T.; Verma, S.C.; Misra, M. Functionalized TiO₂ nanotube-based electrochemical biosensor for rapid detection of SARS-CoV-2. *Sensors* **2020**, *20*, 5871. [[CrossRef](#)]
181. Ramesh, T.; Foo, K.L.; Haarindrapasad, R.; Sam, A.J.; Solayappan, M. Gold-Hybridized Zinc oxide nanorods as Real-time Low-cost nanobiosensors for Detection of virulent DNA signature of HPV-16 in cervical carcinoma. *Sci. Rep.* **2019**, *9*, 17039. [[CrossRef](#)]
182. Bohunicky, B.; Mousa, S.A. Biosensors: The new wave in cancer diagnosis. *Nanotechnol. Sci. Appl.* **2011**, *4*, 1.
183. Shahdeo, D.; Gandhi, S.; Edt: Khan, R.; Parihar, A.; Sangi, S.K. *Next Generation Biosensors as a Cancer Diagnostic Tool (From Lab to Clinic), Biosensor Based Advanced Cancer Diagnostics*; Academic Press: Cambridge, MA, USA; Elsevier Inc.: Amsterdam, The Netherlands, 2022; Chapter 11; pp. 179–196.
184. Liyanage, T.; Alharbi, B.; Quan, L.; Esquela-Kerscher, A.; Slaughter, G. Plasmonic-Based Biosensor for the Early Diagnosis of Prostate Cancer. *ACS Omega* **2022**, *7*, 2411–2418. [[CrossRef](#)]
185. Sohrabi, N.; Valizadeh, A.; Farkhani, S.M.; Akbarzadeh, A. Basics of DNA biosensors and cancer diagnosis. *Artif. Cells Nanomed. Biotechnol.* **2016**, *44*, 654–663. [[CrossRef](#)]
186. Wang, L.; Xiong, Q.; Xiao, F.; Duan, H. 2D nanomaterials based electrochemical biosensors for cancer diagnosis. *Biosens. Bioelectron.* **2017**, *89*, 136–151. [[CrossRef](#)] [[PubMed](#)]
187. Condrat, C.E.; Dana Claudia Thompson, D.C.; Barbu, M.G.; Bugnar, O.L.; Boboc, A.; Cretoiu, D.; Suci, N.; Cretoiu, S.M.; Voinea, S.C. miRNAs as Biomarkers in Disease: Latest Findings Regarding Their Role in Diagnosis and Prognosis. *Cells* **2020**, *9*, 276. [[CrossRef](#)]
188. Rasooly, A.; Jacobson, J. Development of biosensors for cancer clinical testing. *Biosens. Bioelectron.* **2006**, *21*, 1851–1858. [[CrossRef](#)] [[PubMed](#)]
189. Armelao, L.; Pascolini, M.; Biasiolo, E.; Tondello, E.; Bottaro, G.; Dalle Carbonare, M.; D'Arrigo, A.; Leon, A. Innovative metal oxide-based substrates for DNA microarrays. *Inorganica Chim. Acta* **2008**, *361*, 3603–3608. [[CrossRef](#)]
190. Taitt, C.R.; Anerson, G.P.; Ligler, F.S. Evanescent wave fluorescence biosensors. *Biosens. Bioelectron.* **2005**, *20*, 2470–2487. [[CrossRef](#)]
191. Li, M.; Jiang, F.; Xue, L.; Peng, C.; Shi, Z.; Zhang, Z.; Li, J.; Pan, Y.; Wang, X.; Feng, C.; et al. Recent Progress in Biosensors for Detection of Tumor Biomarkers. *Molecules* **2022**, *27*, 7327. [[CrossRef](#)]
192. Zhao, J.; Wang, S.; Zhang, S.; Zhao, P.; Wang, J.; Yan, M.; Ge, S.; Yu, J. Peptide cleavage-mediated photoelectrochemical signal on-off via CuS electronic extinguisher for PSA detection. *Biosens. Bioelectron.* **2020**, *150*, 111958. [[CrossRef](#)]
193. Li, H.; Xiao, Q.; Lv, J.; Lei, Q.; Huang, Y. Dopamine modified hyperbranched TiO₂ arrays based ultrasensitive photoelectrochemical immunosensor for detecting neuron specific enolase. *Anal. Biochem.* **2017**, *531*, 48–55. [[CrossRef](#)]
194. Zhang, Y.; Wu, T.; Liu, D.; Xu, R.; Ma, H.; Wei, Q.; Zhang, Y. Photoelectrochemical immunosensor for the sensitive detection of neuron-specific enolase based on the effect of Z-scheme WO₃/NiCo₂O₄ nanoarrays p-n heterojunction. *Biosens. Bioelectron.* **2022**, *213*, 114452. [[CrossRef](#)]
195. Xu, Q.; Liang, K.; Liu, R.-Y.; Deng, L.; Zhang, M.; Shen, L.; Liu, Y.-N. Highly sensitive fluorescent detection of p53 protein based on DNA functionalized Fe₃O₄ nanoparticles. *Talanta* **2018**, *187*, 142–147. [[CrossRef](#)] [[PubMed](#)]
196. Wang, H.; Wang, Y.; Zhang, Y.; Wang, Q.; Ren, X.; Wu, D.; Wei, Q. Photoelectrochemical Immunosensor for Detection of Carcinoembryonic Antigen Based on 2D TiO₂ Nanosheets and Carboxylated Graphitic Carbon Nitride. *Sci. Rep.* **2016**, *6*, 27385. [[CrossRef](#)] [[PubMed](#)]
197. Luo, J.; Liang, D.; Li, X.; Liu, S.; Deng, L.; Ma, F.; Wang, Z.; Yang, M.; Chen, X. Photoelectrochemical detection of human epidermal growth factor receptor 2 (HER2) based on Co₃O₄-ascorbic acid oxidase as multiple signal amplifier. *Mikrochim. Acta* **2021**, *188*, 166. [[CrossRef](#)] [[PubMed](#)]
198. Adam, T.; Gopinath, S.C. Nanosensors: Recent Perspectives on Attainments and Future Promise of Downstream Applications. *Process Biochem.* **2022**, *117*, 153–173. [[CrossRef](#)]
199. Xia, Y.; Huang, W.; Zheng, J.; Niu, Z.; Li, Z. Nonenzymatic amperometric response of glucose on a nanoporous gold film electrode fabricated by a rapid and simple electrochemical method. *Biosens. Bioelectron.* **2011**, *26*, 3555–3561. [[CrossRef](#)]
200. Manasa, G.; Raj, C.; Satpati, A.K.; Mascarenhas, R.J. S (O) MWCNT/modified carbon paste—A non-enzymatic amperometric sensor for direct determination of 6-mercaptopurine in biological fluids. *Electroanalysis* **2020**, *32*, 2431–2441. [[CrossRef](#)]
201. Hussain, M.M.; Asiri, A.M.; Uddin, J.; Rahman, M.M. An enzyme free simultaneous detection of γ -amino-butyric acid and testosterone based on copper oxide nanoparticles. *RSC Adv.* **2021**, *11*, 20794–20805. [[CrossRef](#)]
202. Zhu, C.; Yang, G.; Li, H.; Du, D.; Lin, Y. Electrochemical sensors and biosensors based on nanomaterials and nanostructures. *Anal. Chem.* **2015**, *87*, 230–249. [[CrossRef](#)]
203. Curulli, A. Nanomaterials in electrochemical sensing area: Applications and challenges in food analysis. *Molecules* **2020**, *25*, 5759. [[CrossRef](#)]

204. Rahman, M.M.; Hussain, M.M.; Ashiri, A.M. Bilirubin sensor based on CuO-CdO composites deposited in a nafion/glassy carbon electrode matrixes. *Prog. Nat. Sci. Mater. Int.* **2017**, *27*, 566–573. [[CrossRef](#)]
205. Rahman, M.M.; Alam, M.M.; Asiri, A.M.; Opo, F. An Electrochemical Approach for the Selective Detection of Cancer Metabolic Creatine Biomarker with Porous Nano-Formulated CMNO Materials Decorated Glassy Carbon Electrode. *Sensors* **2020**, *20*, 7060. [[CrossRef](#)] [[PubMed](#)]
206. Ronkainen, N.J.; Halsall, H.B.; Heineman, W.R. Electrochemical biosensors. *Chem. Soc. Rev.* **2010**, *39*, 1747–1763. [[CrossRef](#)] [[PubMed](#)]
207. Putzbach, W.; Ronkainen, N.J. Immobilization techniques in the fabrication of nanomaterial-based electrochemical biosensors: A review. *Sensors* **2013**, *13*, 4811–4840. [[CrossRef](#)] [[PubMed](#)]
208. Whitcombe, M.J.; Kirsch, N.; Nicholls, I.A. Molecular imprinting science and technology: A survey of the literature for the years 2004–2011. *J. Mol. Recognit.* **2014**, *27*, 297–401.
209. Movlaee, K.; Ganjali, M.R.; Norouzi, P.; Neri, G. Iron-based nanomaterials/graphene composites for advanced electrochemical sensors. *Nanomaterials* **2017**, *7*, 406. [[CrossRef](#)]
210. Kassirer, J.P. Clinical evaluation of kidney function: Glomerular function. *N. Engl. J. Med.* **1971**, *285*, 355–389. [[CrossRef](#)]
211. Neri, G. Solid state gas sensors for clinical diagnosis. In *Biological and Medical Sensor Technologies*; Iniewski, K., Ed.; CRC Press: Boca Raton, FL, USA, 2012; pp. 201–226.
212. Levey, A.; Coresh, S. Chronic kidney disease. *Lancet* **2012**, *379*, 165–180. [[CrossRef](#)]
213. Van Veldhuisen, D.J.; Ruilope, L.M.; Maisel, A.S.; Damman, K. Biomarkers of renal injury and function: Diagnostic, prognostic and therapeutic implications in heart failure. *Eur. Heart J.* **2016**, *37*, 2577–2585. [[CrossRef](#)]
214. Johnson, R.J.; Nakagawa, T.; Jalal, D.; Sánchez-Lozada, L.G.; Kang, D.H.; Ritz, E. Uric acid and chronic kidney disease: Which is chasing which? *Nephrol. Dial. Transplant.* **2013**, *28*, 2221–2228. [[CrossRef](#)]
215. Kosugi, T.; Nakayama, T.; Heinig, M.; Zhang, L.; Yuzawa, Y.; Sanchez-Lozada, L.G.; Roncal, C.; Johnson, R.J.; Nakagawa, T. Effect of lowering uric acid on renal disease in the type 2 diabetic db/db mice. *Am. J. Physiol.-Ren. Physiol.* **2009**, *297*, F481–F488. [[CrossRef](#)]
216. Mazzali, M.; Kim, Y.G.; Suga, S.I.; Gordon, K.L.; Kang, D.H.; Jefferson, J.A.; Hughes, J.; Kivlighn, S.D.; Lan, H.Y.; Johnson, R.J. Hyperuricemia exacerbates chronic cyclosporine nephropathy. *Transplantation* **2001**, *71*, 900–905. [[CrossRef](#)] [[PubMed](#)]
217. Mazali, F.C.; Johnson, R.J.; Mazzali, M. Use of uric acid-lowering agents limits experimental cyclosporine nephropathy. *Nephron. Exp. Nephrol.* **2012**, *120*, e12–e19. [[CrossRef](#)] [[PubMed](#)]
218. Karimi-Maleh, H.; Arotiba, O.A. Simultaneous determination of cholesterol, ascorbic acid and uric acid as three essential biological compounds at a carbon paste electrode modified with copper oxide decorated reduced graphene oxide nanocomposite and ionic liquid. *J. Colloid Interface Sci.* **2020**, *560*, 208–212. [[CrossRef](#)] [[PubMed](#)]
219. Buledi, J.A.; Ameen, S.; Memon, S.A.; Fatima, A.; Solangi, A.R.; Mallah, A.; Karimi, F.; Malakmohammadi, S.; Agarwal, S.; Gupta, V.K. An improved non-enzymatic electrochemical sensor amplified with CuO nanostructures for sensitive determination of uric acid. *Open Chem.* **2021**, *19*, 481–491. [[CrossRef](#)]
220. Sharma, A.; Faber, H.; AlGhamdi, W.S.; Naphade, D.; Lin, Y.H.; Heeney, M.; Anthopoulos, T.D. Label-Free Metal-Oxide Transistor Biosensors for Metabolite Detection in Human Saliva. *Adv. Sci.* **2024**, *11*, 2306038. [[CrossRef](#)]
221. Rahman, M.M.; Alam, M.M.; Alamry, K.A. A reliable alternative approach for the ultra-sensitive detection of l-glutathione with wet chemically synthesized Co₃O₄-doped SnO₂ nanoparticles decorated on a glassy carbon electrode. *New J. Chem.* **2020**, *44*, 16020–16030. [[CrossRef](#)]
222. Ansari, S.A.; Ahmed, A.; Ferdousi, F.K.; Salam, M.A.; Shaikh, A.A.; Barai, H.R.; Lopa, N.S.; Rahman, M.M. Conducting poly (aniline blue)-gold nanoparticles composite modified fluorine-doped tin oxide electrode for sensitive and non-enzymatic electrochemical detection of glucose. *J. Electroanal. Chem.* **2019**, *850*, 113394. [[CrossRef](#)]
223. Wu, H.X.; Cao, W.M.; Li, Y.; Liu, G.; Wen, Y.; Yang, H.F.; Yang, S.P. In situ growth of copper nanoparticles on multiwalled carbon nanotubes and their application as non-enzymatic glucose sensor materials. *Electrochim. Acta* **2010**, *55*, 3734–3740. [[CrossRef](#)]
224. Rahman, M.M.; Adeosun, W.A.; Asiri, A.M. Fabrication of selective and sensitive chemical sensor development based on flower-flake La₂ZnO₄ nanocomposite for effective non-enzymatic sensing of hydrogen peroxide by electrochemical method. *Microchem. J.* **2020**, *159*, 105536. [[CrossRef](#)]
225. Chen, G.; Zheng, J. Non-enzymatic electrochemical sensor for nitrite based on a graphene oxide–polyaniline–Au nanoparticles nanocomposite. *Microchem. J.* **2021**, *164*, 106034. [[CrossRef](#)]
226. Duan, C.; Bai, W.; Zheng, J. Non-enzymatic sensors based on a glassy carbon electrode modified with Au nanoparticles/polyaniline/SnO₂ fibrous nanocomposites for nitrite sensing. *New J. Chem.* **2018**, *42*, 11516–11524. [[CrossRef](#)]
227. Lu, W.; Sun, Y.; Dai, H.; Ni, P.; Jiang, S.; Wang, Y.; Li, Z.; Li, Z. Fabrication of cuprous sulfide nanorods supported on copper foam for nonenzymatic amperometric determination of glucose and hydrogen peroxide. *RSC Adv.* **2016**, *6*, 90732–90738. [[CrossRef](#)]
228. Bolat, G.; Abaci, S. Non-enzymatic electrochemical sensing of malathion pesticide in tomato and apple samples based on gold nanoparticles-chitosan-ionic liquid hybrid nanocomposite. *Sensors* **2018**, *18*, 773. [[CrossRef](#)]

229. Chen, Y.C.; Hsu, J.H.; Chen, Z.B.; Lin, Y.G.; Hsu, Y.K. Fabrication of Fe₃O₄ nanotube arrays for high-performance non-enzymatic detection of glucose. *J. Electroanal. Chem.* **2017**, *788*, 144–149. [\[CrossRef\]](#)
230. Rashed, M.A.; Ahmed, J.; Faisal, M.; Alsareii, S.A.; Jalalah, M.; Tirth, V.; Harraz, F.A. Surface modification of CuO nanoparticles with conducting polythiophene as a non-enzymatic amperometric sensor for sensitive and selective determination of hydrogen peroxide. *Surf. Interfaces* **2022**, *31*, 101998. [\[CrossRef\]](#)
231. Song, C.; Yang, X.; Wang, K.; Wang, Q.; Huang, J.; Liu, J.; Liu, W.; Liu, P. Label-free and non-enzymatic detection of DNA based on hybridization chain reaction amplification and dsDNA-templated copper nanoparticles. *Anal. Chim. Acta* **2014**, *827*, 74–79. [\[CrossRef\]](#)
232. Kumar, P.; Lambadi, P.R.; Navani, N.K. Non-enzymatic detection of urea using unmodified gold nanoparticles based aptasensor. *Biosens. Bioelectron.* **2015**, *72*, 340–347. [\[CrossRef\]](#)
233. Maheshwaran, S.; Chen, W.H.; Lin, S.L.; Ghorbani, M.; Hoang, A.T. Metal oxide-based electrochemical sensors for pesticide detection in water and food samples: A review. *Environ. Sci. Adv.* **2024**, *3*, 154. [\[CrossRef\]](#)
234. Kannan, P.; Maduraiveeran, G. Metal Oxides Nanomaterials and Nanocomposite-Based Electrochemical Sensors for Healthcare Applications. *Biosensors* **2023**, *13*, 542. [\[CrossRef\]](#)
235. Keles, G.; Sifa Ataman, E.; Taskin, S.B.; Polatoglu, I.; Kurbanoglu, S. Nanostructured Metal Oxide-Based Electrochemical Biosensors in Medical Diagnosis. *Biosensors* **2024**, *14*, 238. [\[CrossRef\]](#)
236. Kumar, P.; Rajan, R.; Upadhyaya, K.; Behl, G.; Xiang, X.X.; Huo, P.; Liu, B. Metal oxide nanomaterials based electrochemical and optical biosensors for biomedical applications: Recent advances and future prospectives. *Environ. Res.* **2024**, *247*, 118002. [\[CrossRef\]](#) [\[PubMed\]](#)
237. Rocchitta, G.; Spanu, A.; Babudieri, S.; Latte, G.; Madeddu, G.; Galleri, G.; Nuvoli, S.; Bagella, P.; Demartis, M.I.; Fiore, V.; et al. Enzyme biosensors for biomedical applications: Strategies for safeguarding analytical performances in biological fluids. *Sensors* **2016**, *16*, 780. [\[CrossRef\]](#) [\[PubMed\]](#)
238. Drescher, D.G.; Selvakumar, D.; Drescher, M.J. Analysis of protein interactions by surface plasmon resonance. *Adv. Protein Chem. Struct. Biol.* **2018**, *110*, 1–30. [\[PubMed\]](#)
239. Padiglia, A.; Medda, R.; Lorrain, A.; Paci, M.; Pedersen, J.Z.; Boffi, A.; Agrò, A.F.; Floris, G. Irreversible inhibition of pig kidney copper-containing amine oxidase by sodium and lithium ions. *Eur. J. Biochem.* **2001**, *268*, 4686–4697. [\[CrossRef\]](#)
240. Lin, L.L.; Lu, B.Y.; Chi, M.C.; Huang, Y.F.; Lin, M.G.; Wang, T.F. Activation and thermal stabilization of a recombinant γ -glutamyltranspeptidase from *Bacillus licheniformis* ATCC 27811 by monovalent cations. *Appl. Microbiol. Biotechnol.* **2022**, *106*, 1991–2006. [\[CrossRef\]](#)
241. Medjidov, A.A.; Ismayilova, S.Z.; Ganzayeva, G.M.; Agaeva, S.A.; Qasimova, S.N. Properties of polymers based on aromatic diamines. *Azerbaijan Chem. J.* **2022**, *3*, 21–44. [\[CrossRef\]](#)
242. Avelino, K.Y.; Oliveira, L.S.; Santos, M.R.; Lucena-Silva, N.; Andrade, C.A.; Oliveira, M.D. Electrochemical dna biosensor for chronic myelocytic leukemia based on hybrid nanostructure. *Bioelectrochemistry* **2022**, *147*, 108176. [\[CrossRef\]](#)
243. Altug, H.; Oh, S.H.; Maier, S.A.; Homola, J. Advances and applications of nanophotonic biosensors. *Nat. Nanotechnol.* **2022**, *17*, 5–16. [\[CrossRef\]](#)
244. Oliverio, M.; Perotto, S.; Messina, G.C.; Lovato, L.; De Angelis, F. Chemical functionalization of plasmonic surface biosensors: A tutorial review on issues, strategies, and costs. *ACS Appl. Mater. Interfaces* **2017**, *9*, 29394–29411. [\[CrossRef\]](#)
245. Shrivastava, S.; Trung, T.Q.; Lee, N.E. Recent progress, challenges, and prospects of fully integrated mobile and wearable point-of-care testing systems for self-testing. *Chem. Soc. Rev.* **2020**, *49*, 1812–1866. [\[CrossRef\]](#)
246. Lopez, G.A.; Estevez, M.C.; Soler, M.; Lechuga, L.M. Recent advances in nanoplasmonic biosensors: Applications and lab-on-a-chip integration. *Nanophotonics* **2017**, *6*, 123–136. [\[CrossRef\]](#)
247. Zanchetta, G.; Lanfranco, R.; Giavazzi, F.; Bellini, T.; Buscaglia, M. Emerging applications of label-free optical biosensors. *Nanophotonics* **2017**, *6*, 627–645. [\[CrossRef\]](#)
248. Yesilkoy, F.; Terborg, R.A.; Pello, J.; Belushkin, A.A.; Jahani, Y.; Pruneri, V.; Altug, H. Phase-sensitive plasmonic biosensor using a portable and large field-of-view interferometric microarray imager. *Light Sci. Appl.* **2018**, *7*, 17152. [\[CrossRef\]](#) [\[PubMed\]](#)
249. Shi, X.; Gu, W.; Li, B.; Chen, N.; Zhao, K.; Xian, Y. Enzymatic biosensors based on the use of metal oxide nanoparticles. *Microchim. Acta* **2014**, *181*, 1–22. [\[CrossRef\]](#)

Disclaimer/Publisher's Note: The statements, opinions and data contained in all publications are solely those of the individual author(s) and contributor(s) and not of MDPI and/or the editor(s). MDPI and/or the editor(s) disclaim responsibility for any injury to people or property resulting from any ideas, methods, instructions or products referred to in the content.